Polymer Journal (2022) 54:427–453
https://doi.org/10.1038/s41428-021-00587-8

REVIEW

Specific β-glucans in chain conformations and their biological functions

Huanhuan Chen[1] · Ningyue Liu[1] · Fangzhou He[1] · Qingye Liu[2] · Xiaojuan Xu[1,3]

Received: 18 September 2021 / Revised: 20 October 2021 / Accepted: 21 October 2021 / Published online: 8 January 2022

Abstract

The structures and functions of polysaccharides are not fully understood by the scientific community due to their complexity and the limitations of characterization methods. β-(1,3)-D-glucans with or without β-(1,6)-linked glucopyranans as branches (β-glucans), which are important polysaccharides, are widely involved in various biological activities. Moreover, β-glucans exhibit a strong ability to self-assemble into diverse nanocomposite biomaterials, showing great promise in the diagnosis and therapeutic treatment of human diseases. Fungi are well known for their traditional edible and medical value, and β-glucans are one of the major active components in fungi. We have long been committed to the study of the structure and function of β-glucans from edible mushrooms, especially in the biological and food fields. Hence, research advances in the extraction, structural and conformational characteristics, and biological activities of β-glucans from three fungi, *Auricularia auricula judae*, *Lentinus edodes* and yeast, as typical representatives, were the focus of this review article. Additionally, as-fabricated β-glucan-derived nanocomposite biomaterials as effective therapeutic agents were addressed. This review provides a more comprehensive understanding of β-glucans and some valuable insights for research regarding other polysaccharides.

Introduction

Naturally occurring polysaccharides are the third most important biomacromolecules after DNA and proteins since they widely exist in living bodies and play diverse and important roles in many biological processes, such as cell recognition, biological information transfer, metabolism, and immune response regulation [1–3]. However, polysaccharides have not received sufficient attention for a long time due to the complexity and diversity of their structures and existing states. With the development of technologies for isolation, purification, characterization and analysis by molecular biology, polysaccharides from a variety of sources have attracted increasing attention due to their plentiful pharmacological properties, such as anti-tumor, anti-inflammatory, antidiabetic and immunological effects [4–7], which open a pathway to a class of new and improved therapeutics, as well as the next frontier in pharmaceutical research [8]. Moreover, owing to their strong associations and interactions resulting from the hydrophobicity of sugar rings and hydrogen bonding between hydroxyl groups, polysaccharides can even self-assemble into ordered structures such as nanotubes [9] and vesicles [10]. In combination with the outstanding inherent properties of bioactivity, biodegradability, biocompatibility, low cost, and availability, polysaccharides show great potential in biomaterials, particularly in drug/gene delivery, bioimaging and tissue engineering [11].

Among a variety of polysaccharides, specific polysaccharides demonstrating a common bonding mode with β-(1,3)-glucans as the backbone and with or without β-(1,6)-linked glucopyranans as branches are called β-glucans herein. Several well-known β-glucans have been discovered,

These authors contributed equally: Huanhuan Chen, Ningyue Liu, Fangzhou He

✉ Qingye Liu
qingyeliu@126.com

✉ Xiaojuan Xu
xuxj@whu.edu.cn

[1] College of Chemistry and Molecular Sciences, Wuhan University, Wuhan 430072, China

[2] School of Chemical Engineering and Technology, North University of China, NO. 3 Xueyuan Road, Jiancaoping District, Taiyuan 030051, China

[3] Hubei Engineering Center of Natural Polymers-based Medical Materials, Wuhan University, Wuhan 430072, China

such as curdlan of the linear β-(1,3)-glucan produced from *Acaligenes faecalis var. myxogene* and other microorganisms [12, 13], schizophyllan produced by *Schizophyllum commune* [14], scleroglucan secreted by the fungus *Sclerotium glucanicum*, yeast β-glucan produced by *Saccharomyces cerevisiae* [15], and lentinan extracted from the fungus *Lentinus edodes* [16]. These β-glucans have different water solubilities depending on the branching degree of β-(1,6)-linkages. In general, linear β-(1,3)-glucans with few or no β-(1,6)-branches, such as curdlan [12] and yeast β-glucan [17], are usually water-insoluble, while β-(1,6)-branched β-(1,3)-glucans, such as schizophyllan [18], scleroglucan [19] and lentinan [20], can be dissolved in water. It is noted that their high-molecular weight is the key factor affecting the water solubility of β-glucans. For example, lentinan with a high-molecular weight forms gels in water due to its low water solubility [21]. It is interesting that all of these β-glucans adopt a unique conformation of a triple helix in nature or in water [22], which has been demonstrated by using X-ray diffraction [23], laser light scattering and viscometry in combination with polymer solution theories such as the cylinder model, touched-bead model and Benoit-Doty equation. Notably, β-glucans can bind to membrane receptors such as dectin-1, complement receptor 3 (CR3), and Toll-like receptors (TLRs) to activate immunocytes, leading to subsequent immunoregulation and an enhanced innate immune response to infection [24]. Therefore, β-glucans have been used as immunomodulators, as well as in the treatment of cancer or inflammation [25–27]. For example, schizophyllan and lentinan have been used as adjuvants to treat patients bearing tumors in Asian countries [28, 29]. It is predicted that pharmacotherapy using natural β-glucans with good biocompatibility will be a better alternative than conventional therapy.

Benefitting from their unique triple helical structure characteristics and favorable affinity to immune cells, β-glucans have been manipulated into diverse nanostructured biomaterials with high performance in theranostics and an integrated approach of therapeutics and diagnostics. For instance, schizophyllan has been introduced as a soft matrix to accommodate inorganic nanoparticles [30], fluorescent dyes [31], single-walled carbon nanotubes [32], conducting polymers [33] and genes [34] for versatile therapeutic functions. The adjustable one-dimensional hydrophobic nanocavity of triplex β-glucans [35], the native microcavity in yeast particles [36], or the well defined hollow nanofibers generated by self-assembly of stiff chains [37] can easily encapsulate host guests, creating more multimodal and multifunctional systems for biomedical use. These "sugar" coatings endow hybrid biomaterials with several advantages in in vivo delivery and tumor targeting, including longer circulation time, easier stabilization and functionalization, higher cellular uptake, more specific targeting, and lower long-term toxicity. More interestingly, the single chains released from the triple helical β-glucans can be reassociated into a triple helix and even form a heterotriplex with specific homo-polynucleotides, such as poly(cytidylic acid) (poly(C)), poly(adenylic acid) (poly(A)), poly(uracil acid) (poly(U)), poly(thymidine acid) (poly(T)) and poly(deoxyadenylic acid) (poly(dA)), consisting of two single polysaccharide chains and a single polynucleotide chain [38–40]. This discovery paves the way for the development of gene delivery [41–43]. For example, a nanoplatform constructed from single chains of lentinan and poly(dA) has been proven to be a promising strategy for the effective delivery of genes targeting intestinal inflammation, where the target gene is attached to the tail of poly(dA) through a disulfide bond and is eventually internalized by macrophages for further expression in a triggered manner [44].

Based on these findings, studies of the structures and roles of polysaccharides in cells are very important to clarify the mystery of polysaccharides such as β-glucans in life-associated activities. Despite their key roles in a broad range of biological processes, including transduction and immune responses, β-glucans have still been underappreciated by the scientific community due to their complex structures compared with proteins and nucleic acids. Fungi are well known for their traditional edible and medical value, and polysaccharides are one of the major active components. To clarify the chain or higher order structure and discover more unknown functions of polysaccharides, especially in the biological and food fields, our research interests have focused on the chain conformation, multiscale structure and biological functions of β-glucans from fungi such as *Auricularia auricula*, *Lentinus edodes* and yeast, which are usually used in our daily diets. In this review, the extraction, structural/conformational features, and biological functions of three β-glucans were summarized, and the development of β-glucan-derived nanocomposite biomaterials as effective therapeutic agents was emphasized. This review will provide valuable insights and important guidance for researchers or developers to better use β-glucans as functional products with nutritional and biological effects that benefit human health.

β-glucan from Auricularia auricula

Extraction and structure of β-glucan from *Auricularia auricula judae*

Auricularia auricula judae (AAJ) belongs to the genus *Auricularia* of *Basidiomycetes*, *Auriculariaceae*, which is mainly distributed in the temperate regions of the Northern Hemisphere shade area. It is popularly known as a precious medicinal and edible fungus in many countries due to its

rich nutrition and delicacy. Polysaccharides are one of the main active components of AAJ. The types of polysaccharides originating from AAJ strongly rely on the extraction conditions. The most common extraction method is solvent extraction by using hot water or alkali solution, which is usually carried out in combination with several physically assisted extraction methods, including microwave, ultrasonic, and pulsed electric field or ultrahigh temperature/pressure extraction, to enhance productivity [45–48]. The different strategies result in different monosaccharide components and molecular weights, finally leading to different bioactivities. Heteropolysaccharides are usually extracted from AAJ. For example, Ma and Zhang acquired a kind of water-soluble polysaccharide by utilizing a 70% ethanol/water solvent system, which was composed of the main chain of β-(1,4)-linked D-glucopyranan with D-glucopyranan as the side group at O6 and 19% glucuronic acid [49]. Another water-soluble acidic heteropolysaccharide was separated from AAJ by extraction with 0.9% aqueous NaCl solution, which has a backbone of α-(1,3)-linked D-mannopyranose residues with pendant side groups of β-D-xylose, β-D-glucose, or β-D-glucuronic acid at position O6 or O2, exhibiting the characteristic of a semirigid linear chain in aqueous solution [50]. Few studies have dealt with β-glucans in AAJ.

Recently, a water-soluble neutral β-glucan was successfully extracted from AAJ with the aid of 0.15 M NaCl aqueous solution at 80~100 °C, which was denoted as AF1 [51] or BFP [9]. The yield is estimated to be ~1%, much lower than that for heteropolysaccharides in AAJ [52, 53]. Its chemical structure was identified as a β-(1,3)-D-glucan with two β-(1,6)-linked D-glucopyranans for every three D-glucopyranans in the main chain, showing a comb-branched structure by using gas chromatography (Fig. 1) in combination with mass chromatography and NMR [51, 54]. Compared with schizophyllan and scleroglucan, AF1 or BFP has a higher β-(1,6)-branching degree. The structural features of AF1 are shown in Table 1.

Triple helical chain conformation of β-glucan from AAJ

The chain conformation of polysaccharides is closely related to their biological functions. Identification of the chain conformation and regulation of the chain conformation transition are essential for the successful application of polysaccharides in food and medical fields. Natural polysaccharides show conformations such as random coils, semiflexible chains, double helices, triple helices and aggregates [55]. Generally, the chain conformation can be deduced by conformational parameters such as persistence length (q), chain diameter (d), contour length (L), and molar mass per unit contour length (M_L), which are estimated from

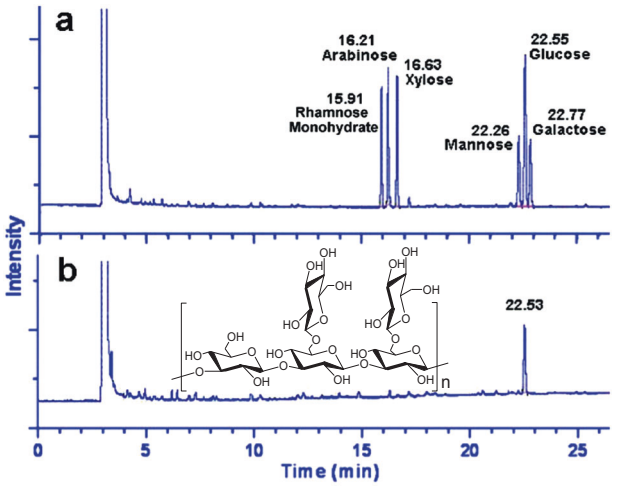

Fig. 1 GC traces of monosaccharide standards (**a**) and the hydrolyzed products of polysaccharides from the fruiting bodies of *Auricularia auricula judae* (AF1) (**b**). The inset in **b** is the chemical structure of AF1 [51]. Copyright © 2012, American Chemical Society

weight-average molecular weight (M_w), radius of gyration (R_g), and hydrodynamic radius (R_h) in combination with polymer solution theories and even directly observed by atomic force microscopy (AFM) and transmission electron microscopy (TEM).

AF1 was first proven to adopt a stiff chain conformation in water by using the value of the structure-sensitive parameter ρ ($\equiv R_g/R_h$), which was estimated to be 2.3 [51]. To further clarify the chain conformation, 9 fractions of AF1 with different molecular weights were prepared by ultrasonication and ethanol precipitation, and the values of M_w, R_g and [η] were determined using laser light scattering and viscometry [54]. The dependences of R_g and [η] on M_w were $[\eta] = 1.78 \times 10^{-7} M_w^{1.6}$ (mL/g) (Fig. 2a) and $R_g = 5 \times 10^{-4} M_w^{0.9}$ (nm), respectively (Fig. 2b). The high exponents of 1.6 and 0.9 indicate that AF1 adopts a rod-like chain conformation in water. The M_L, q, d and helix pitch distance (h) were calculated to be 2724 ± 276 nm, 230 ± 30 nm, ~2.2 nm and ~0.37 nm, respectively, with the wormlike chain model [54], similar to the conformational parameter values of triple helical schizophyllan [56] and scleroglucan [57]. Moreover, the value of M_w in dimethyl sulfoxide (DMSO) is ~1/3 of that in water. In combination with the conformational parameters and the molecular weight changes, it is thus concluded that AF1 exists as a triple-helix conformation in water and single chains in DMSO.

Simultaneously, molecular dynamics simulations were introduced to determine the chain structures. In the all-atom model, as shown in Fig. 2c–e, two twisting angles of the glycoside bonds on the main chains, Φ (H1–C1–O3–C3) and Ψ (C1–O3–C3–H3), were set to determine the overall structure. The optimized simulation reveals that the potential energy of the triple helix is −256 kcal/mol/ring (at 0 K)

Table 1 Extraction, purification and structural features of β-glucans from different sources

Compound name	Natural source	Name of glycan	Preparation methods	Molecular weight (Da)	Proposed structure	References
AF1/BFP	*Auricularia auricula-judae*	β-D-glucan	0.15 M NaCl aqueous solution at 80~10 ~ 100 °C	2.07×10^6–2.15×10^6	A β-(1,3)-D-glucan with two β-(1,6)-D-glucopyranans for every three main chain D-glucopyranans	[9, 51–54, 62–65]
LNT	*Lentinus edodes*	β-D-glucan	1.25 M NaOH/0.05% $NaBH_4$ aqueous solution	3.01×10^5–1.76×10^6	(1,3)-β-linked D-glucopyranan with two (1,6)-β-linked D-glucopyranans for every five D-glucopyranans	[80, 85, 98]
BYG/BBG	Yeast	Yeast β-glucan	Hot water extraction and Alkali extraction (5% w/v NaOH/0.5% $NaBH_4$)	2.3×10^4–14.8×10^4	A backone of β-(1,3)-glucan with β-(1,6)-branches and minor β-(1,3)-branched β-(1,6)-glucan	[121, 125, 129–132, 134, 135]

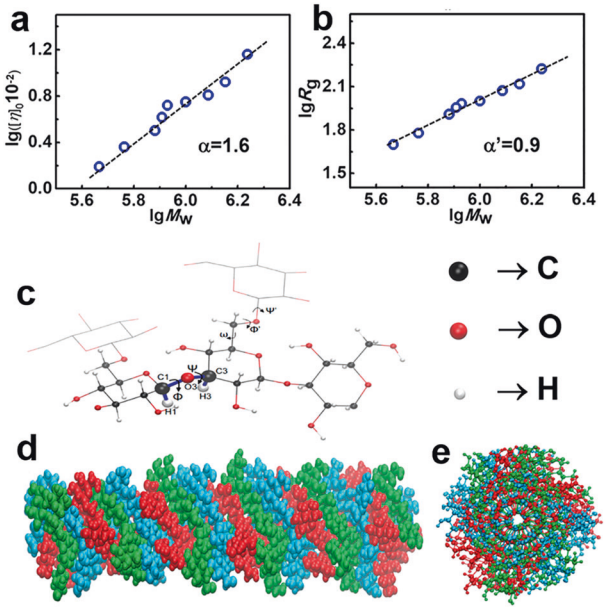

Fig. 2 Double logarithm relationships of $[\eta] \sim M_w$ (**a**) and $R_g \sim M_w$ (**b**). Torsion angles of glycosidic bonds in AF1 (**c**). Structure of triple-helix AF1 in vacuum in the main view (**d**) and the top view (**e**) [54]. Copyright © 2018, American Chemical Society

and −5.6 kcal/mol/ring (at 300 K) in vacuum, indicating that AF1 polymer chains prefer to take a triple-helix conformation in water. In the architecture, three strands are well known to have compacted morphology, and a hydrophobic cavity inside the triple helix is observed, similar to other triple-helix polysaccharides [58, 59].

Biological activity of β-glucan from AAJ

The application of AAJ as a dietary supplement or herbal medicine for health purposes has a long history in Asian countries [60, 61]. Many pharmacological activities of heteropolysaccharides have been revealed, such as activation of macrophages to secrete proinflammatory cytokines by binding to Toll-like receptor-4 (TLR-4) [62], protective activity against radiation by alleviating splenocyte apoptosis and oxidative stress in vitro caused by radiation treatment [63], antitumor activity [64], hypolipidemic activity, anticoagulant activity, synergistic antianemia activity, and antimicrobial activity [60]. However, due to the low yield of β-glucan in AAJ, little attention has been conferred upon it, and its biological activities have seldom been an area of focus. Our latest research reveals that the β-glucan of AF1 exhibits high anti-hepatoma activity and significantly inhibits mouse liver cancer cell (Hepatoma-22, H22) growth without cytotoxicity toward normal tissues [65]. It exhibits both molecular weight- and dosage-dependent antitumor activity, and the β-glucan with a M_w of 7.7×10^5 at the dosage of 5 mg/kg exhibits the highest inhibition ratio of

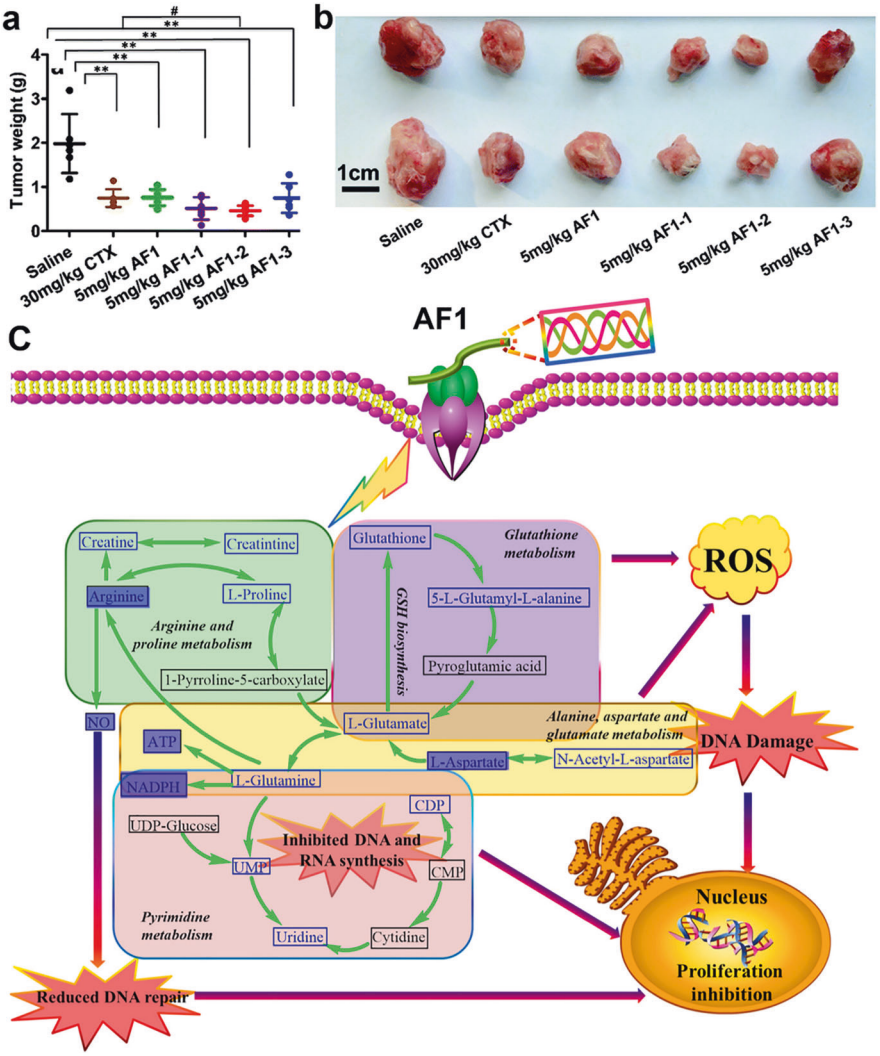

Fig. 3 Anti-hepatoma activities of the AF1, AF1-1, AF1-2 and AF1-3 samples in vivo. The tumor weight is presented in a scatter plot. The bars represent ±SD. *$p < 0.05$, **$p < 0.001$ vs. the saline group, and #$p < 0.05$ vs. the cytoxan (CTX) group. The values of p obtained from statistical analysis represent the difference between the groups. $p < 0.05$ was considered statistically significant (**a**). Representative photographs of the tumor (**b**) [65]. Copyright ©2016 The Royal Society of Chemistry. Schematic depiction of the disturbance of metabolic pathways in HepG2 cells after exposure to AF1. The downregulated metabolites are marked in blue (**c**) [66]. Copyright © 2021 Elsevier Ltd

~77% against H22 tumors, even higher than the positive control of cytoxan (~68%), as depicted in Fig. 3a, b. This occurs because AF1 induces more cytokine/chemokine production by activating immunoresponses and enhances the effect of anti-angiogenesis in tumor tissues. The underlying mechanism was further clarified by employing metabolomic analysis. As illustrated in Fig. 3c, multiple metabolic pathways commonly contribute to the high anti-tumor activity. AF1 induces intracellular oxidative stress and lipid peroxidation and downregulates taurine, glutathione (GSH), energy supply and cellular nicotinamide adenine dinucleotide (NAD^+) generation, thereby giving rise to DNA dysfunction in liver cancer cells [66]. These metabolic behaviors finally inhibit the proliferation, migration and invasion of tumor cells by inducing cell apoptosis and arresting the cell cycle at S phase (DNA synthesis phase), evidently suggesting that AF1 is a potent anticancer candidate for pharmaceutical therapy and providing new insights for pharmacological research and clinical practice for this highly branched β-glucan with a triple helical chain conformation.

Self-assembly behavior and therapeutic application of β-glucan from AAJ

Self-assembly is seldom reported for polysaccharides because random aggregation [20, 67, 68] and gelation are usually observed [69–71]. The study of self-assembly of polysaccharides is a major challenge due to the multiple interactions existing in polysaccharide chains. For the first time, we found that this branched β-glucan of AF1 with a stiff chain conformation displays specific self-orientation and self-assembly behavior in a parallel manner with increasing concentrations [37].

Briefly, AF1 chains first align and assemble into string-like nanofibers at a concentration of 1.3×10^{-6} g/mL due to the strong hydrogen-bonding interactions between polymer chains; with an increase in concentration up to 4×10^{-4} g/mL,

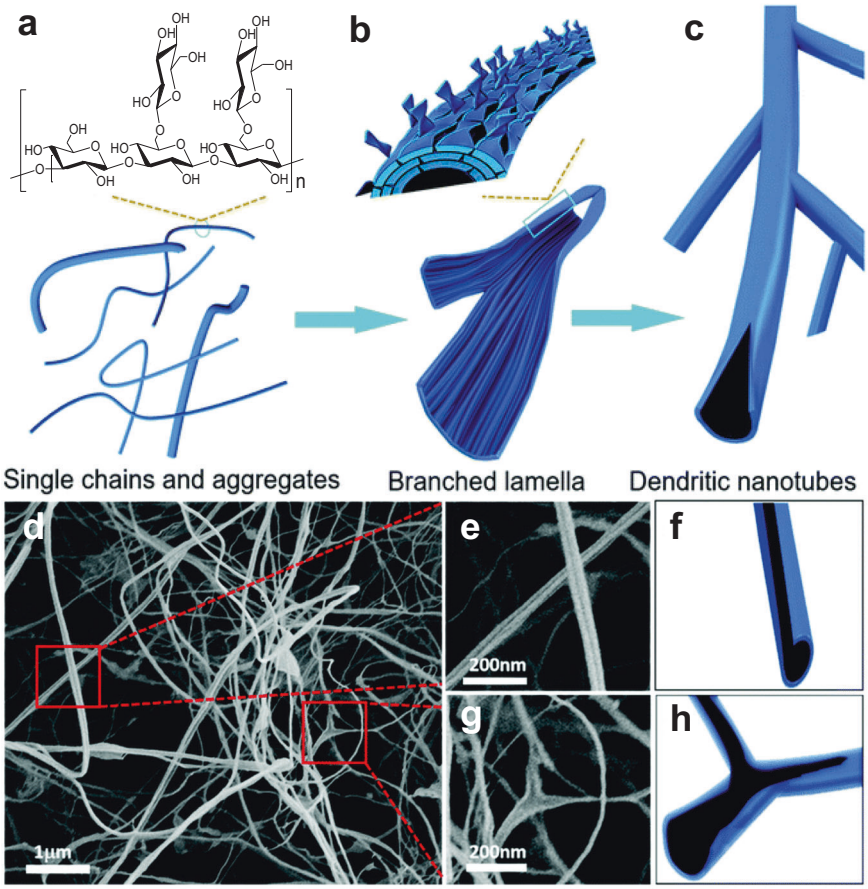

Fig. 4 Schematic diagram of the formation of dendritic nanotubes of β-glucan (AF1-DNTs). The coexistence of single chains and aggregates in AF1 solution (**a**), lamellar aggregates (**b**) and curly dendritic nanotubes (**c**). SEM images of AF1-DNTs obtained by lyophilizing the AF1 solution in liquid nitrogen at a concentration of 0.5 mg/mL (**d**). The magnified images (**e** and **g**) of the red box in **d** and the scheme graphs (**f** and **h**) of **e** and **g** [9]. Copyright © 2017 The Royal Society of Chemistry

AF1 chains tend to form thin lamella and then self-curl into tubular nanofibers with mean diameters from 20 to 80 nm. A higher concentration is beneficial to the formation of nanotubes, and the whole self-assembly process is predicted in the schematic illustration presented in Fig. 4 [9]. The parallel self-orientation is mainly driven by hydrogen bonding and hydrophobic interactions in the polysaccharide backbone. The dense side chains with relative hydrophilicity easily come into contact with water, leading to the arrangement of the hydrophobic backbones inside. Therefore, the nanotubes possess a hydrophobic interior and a relatively hydrophilic exterior.

This unique self-assembly offers great significance since the as-formed hydrophobic cavity can accommodate various guests with hydrophobicity for potential theranostic applications. For example, selenium nanoparticles (SeNPs) with a mean diameter of 46 nm have been successfully entrapped into the cavities of AF1 nanotubes through hydrophobic interactions and the formation of Se–O bonds inside, showing good dispersion and high stability in water for over 16 months. The as-prepared AF1-Se nanocomposites display a broad-spectrum inhibitory effect on human cancers with low half maximal inhibitory concentration values and low toxicity against normal cells. In particular, the inhibition ratio against MCF-7 cancer cells reached ~75% at a concentration of 200 μg/mL (Se content ~29 μM). The antitumor efficiency of this hybrid nanobiomaterial is higher than that of AF1 alone, demonstrating a strong synergistic therapeutic effect. AF1-Se nanocomposites have also been applied for the treatment of acute myeloid leukemia (AML) to test their feasibility. As a result, AF1-Se significantly inhibits the proliferation of AML cells, increases the capacity of total antioxidant AML cells obtained from blood and bone marrow analysis, and decreases the expression of c-Jun activation domain binding protein-1 and thioredoxin-1 [72].

AF1 nanotubes were also used to carry cisplatin, which is a well-known anticancer agent due to its powerful killing effect on cancer cells, but it has serious side effects on normal cells. A favorable strategy is to convert Pt(II) complexes into Pt(IV) prodrugs, where physicochemical properties such as stability, in vivo distribution or targeting ability can be altered by modifying different ligands without changing the pharmacophore core [73, 74]. AF1 nanotubes with hollow cavities were thus chosen to deliver the Pt(IV) prodrug to verify the advantages of this approach. As shown in Fig. 5, the platinum prodrugs can be loaded into the hollow cavity and stabilized through a stable chemical bond, resulting in high stability and good dispersibility in aqueous solution. Simulated release studies confirmed that

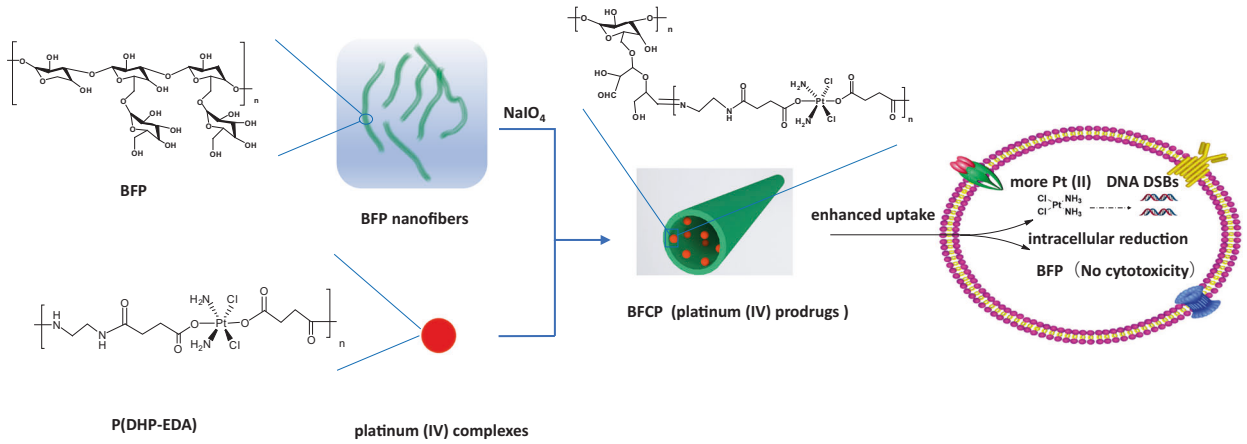

Fig. 5 Schematic illustration of the AF1-Pt nanocomposite and the proposed antitumor mechanism [75]. Copyright © 2021, American Chemical Society

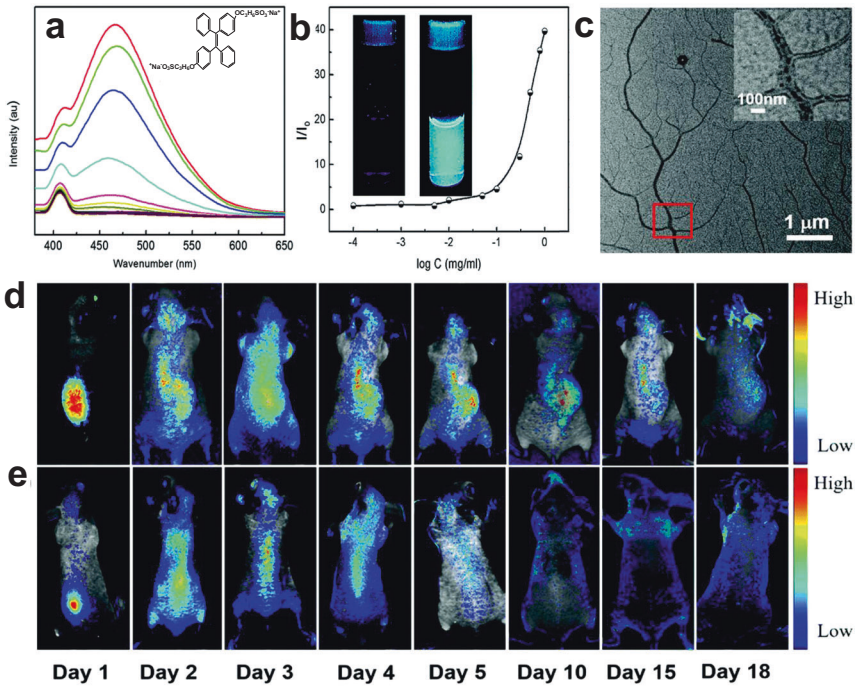

Fig. 6 Changes in the fluorescence intensity of BSPOTPE (1×10^{-6} g/mL) in the presence of AF1 at different concentrations (1×10^{-7} to 1×10^{-3} g/mL) in water (**a**). Relationship of fluorescence intensity at 470 nm versus the concentration of AF1 (0.1 mg/mL) at an excitation wavelength of 350 nm (**b**). The insets in **b** are photographs of BSPOTPE in water (1×10^{-6} g/mL) without (left) and with AF1 (1×10^{-3} g/mL). TEM image of AF1/BSPOTPE (**c**). The inset in **c** is the magnification of the region indicated in red. Fluorescence imaging of nude mice in vivo after subcutaneous injection of 250 mL of AF1/TPA-BMO solution (**d**) and free TPA-BMO solution (**e**). The dye concentration was fixed at 5×10^{-6} g/mL [9]. Copyright © 2017 The Royal Society of Chemistry

the prodrugs convert to Pt(II) by losing axial ligands in biological reducing agents and subsequently platinating DNA. In comparison to cisplatin, Pt(IV) prodrugs display better antitumor properties (50-fold) with specific tumor targeting, providing more references for the development of new antitumor drugs [75].

Based on the structural features of the hydrophobic cavity, the amphiphilic aggregation-induced emission (AIE) molecule 1,2-bis [4-(3-sulfonatopropoxyl) phenyl]-1,2-diphenylethene salt (BSPOTPE) or (Z)-4-benzylidene-2-methyloxazol-5(4H)-one (TPA-BMO) was used for in vivo imaging. As indicated in Fig. 6a–c, the aggregation of AIE molecules embedded in the hollow cavity dramatically enhances the fluorescence intensity with an increase in the concentration of AF1. As a result of the improvement of AIE in water dispersion and cytotoxicity, the TPA-BMO-loaded AF1 nanotubes induce stronger

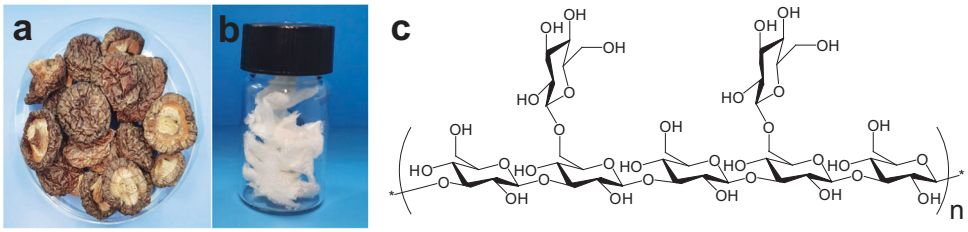

Fig. 7 Pictures of the mushrooms of *Lentinus edodes* (**a**) and lentinan (**b**) and the chemical structure of lentinan (**c**) [85]. Copyright 2012 John Wiley and Sons

fluorescence intensity than TPA-BMO alone and maintain a longer duration time (18 days) in vivo, suggesting a potential candidate for bioimaging [54].

Taken together, AF1 nanotubes are a good candidate to carry nanoparticles, antitumor drugs and imaging agents with biosafety. It is predicted that other guests can also be delivered through AF1 nanotubes. Although some progress has been made in the research on *β*-glucan from AAJ, there are still some key problems that need to be urgently addressed, such as how to sustain and recover the triple helical conformation once it is damaged under harsh conditions. Little is known about the structure-activity relationships of AF1. It is of vital importance to conduct more experiments in vivo and clinical studies to further verify the reliability of AF1 usage. In addition, how to control the morphology parameters of the nanotubes, such as the fibril diameter, length or cavity size, and identification of the key factor determining self-assembly need further study.

β-glucan from Lentinus edodes

Lentinus edodes, similar to *Auricularia auricula judae*, is another popular edible mushroom and has been widely used as a delicious and nutritional food and traditional Chinese medicine in Asia for thousands of years because it contains bioactive compounds such as polysaccharides, proteins, fibers and lipids [76]. Of these, polysaccharides are important active ingredients with various beneficial effects, such as antitumor, antiviral and immunomodulatory activities, allowing them to act as medicinal agents; polysaccharides have been identified as *β*-glucans and are usually named lentinans [77].

Extraction and chemical structure of *β*-glucan from *Lentinus edodes*

Lentinan was first isolated from Shiitake mushroom by Chihara et al. and was demonstrated to show antitumor activity against S-180 solid tumors [78, 79]. The hot water extraction method is a conventional method for extracting lentinan, which produces a low extraction efficiency of less than 0.1%. In our lab, a modified strategy of 1.25 M NaOH/0.05% $NaBH_4$ aqueous solution was well developed with a total polysaccharide yield of more than 3% [80]. Other new technologies, such as supercritical fluid extraction and microwave/ultrasonic/enzymatic-assisted extraction, have also been introduced to enhance the extraction efficiency in recent years. For example, the extraction yield of lentinan from *Lentinus edodes* using microwave-assisted aqueous two-phase extraction based on the Box-Behnken design has been greatly increased and was determined to be 2.12 ± 0.21% and 11.16 ± 0.28% at the top phase and the bottom phase, respectively [81].

The monosaccharide composition and anomerity (*α* or *β*) of each sugar residue were determined by gas chromatography–mass spectrometry (GC–MS), Fourier transform infrared (FT-IR) and nuclear magnetic resonance spectroscopy (NMR) [82–84]. Lentinan has been demonstrated to possess the same backbone chain of *β*-(1,3)-linked D-glucopyranan with two *β*-(1,6)-linked D-glucopyranans for every five D-glucopyranans in the main chain (Fig. 7), yielding a comb-like branched primary structure with water solubility [85]. This repeating unit is slightly different from that of scleroglucan and schizophyllan, which have a *β*-(1,3)-glucan backbone and a *β*-(1,6)-linked D-glucopyranan as side chains at every third D-glucopyranan residue of the main chain [19, 86]. Of course, there are some other polysaccharides with different structures from *β*-glucan. For example, Zhang et al. collected a new water-soluble polysaccharide from *Lentinus edodes*, which is composed of a main chain of (1,4)-linked and (1,3)-linked D-glucopyranan and branches at C-6 of *β*-(1,4)-linked D-glucopyranan [87]. The structures of natural glycans are so diversified that searching for new bioactive polysaccharides is interesting and challenging. The extraction and purification techniques used for the extraction of *β*-glucan from *Lentinus edodes* are summarized in Table 1.

Chain conformation and conformational transition of lentinan

Triple helical chain conformation

It has been reported that lentinan exists in the form of stiff triple helices (denoted as t-LNT) in water and random coils in DMSO using light scattering, size exclusive chromatography and viscometry in combination with polymer solution theories [16]. The established Mark-Houwink-Sakurada equation for

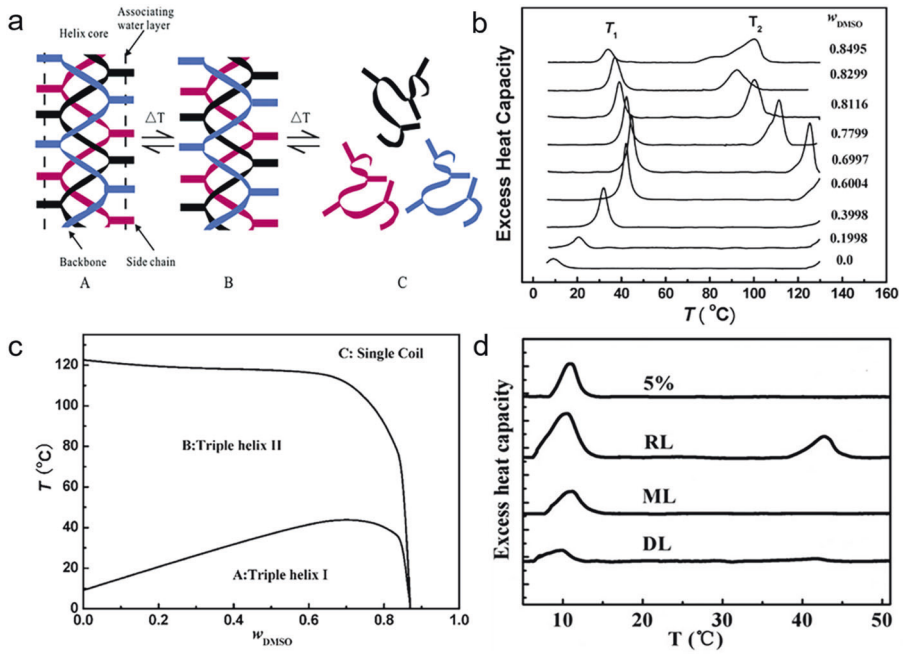

Fig. 8 Schematic diagram of a model describing the conformational transitions of lentinan with temperature in solution (**a**). Temperature dependence of the excess heat capacity for lentinan in DMSO/water mixtures detected by micro-DSC (**b**). Phase diagram for lentinan in DMSO/water mixtures (**c**) [90]. Copyright 2009, American Chemical Society. DSC thermograms for r-LNT against different renaturation modes. RL mode: a large amount of water was added instantaneously into lentinan/DMSO solution; ML mode: water was slowly added into lentinan/DMSO solution at a uniform rate; DL mode: dialysis of lentinan/DMSO solution in water at room temperature (**d**) [85]. Copyright 2012 John Wiley and Sons

t-LNT in 0.5 M NaCl aqueous solution was found to be $[\eta] = 7.69 \times 10^{-6} M_w^{1.32}$ (mL/g). The α value of the exponent in 0.5 M NaCl aqueous solution is far higher than that for lentinan in DMSO (0.73) [88], indicating that lentinan exhibits rigid chains in water and flexibility in DMSO. In the triplex structure, three single chains are connected by interstranded hydrogen-bonding networks among oxygen atoms (O2 and O2') on different x-y planes [59]. Three 2nd hydroxyl groups protrude toward the center of the helical structure and form a hydrophobic cavity in the triangular hydrogen-bonding network. Apart from the individual triple-helical chain, as a result of the strong hydrogen bonding and the small steric hindrance between short triple-helical chains, lentinan with a molecular weight lower than 5.0×10^5 self-compacts in a parallel manner to form "faggot-like" aggregates in aqueous solution [89], suggesting that the ordered structure of lentinan aggregates can be induced by controlling the molecular weight.

Conformational transition at low temperature

The major driving force for maintaining the stability of the helix structure for lentinan is the inter- and intramolecular hydrogen bonds. At temperatures lower than 5 °C, an ordered triple helix (coded as triplex I) with a highly immobile backbone is observed in water due to the intermolecular hydrogen bonding between the associating water layer and the side chain of triple helical lentinan [90]. When the temperature is increased to 5 °C, the hydrogen-bonding network can be broken easily, leading to the free rotation of the side chains on the backbone of the triple helix (coded as triplex II) (Fig. 8a). This conformational transition is a reversible conformational transition from triplex I to triplex II at lower temperatures. Interestingly, this conformation transition temperature (T_1, shown in Fig. 8b) strongly depends on the ratio of DMSO in the mixed aqueous solution. As indicated, when the weight ratio of DMSO (w_{DMSO}) in water was lower than 0.70, lentinan changed from triplex I to relatively free triple helix II with an increase in temperature from 8 to 45 °C.

Triple helix-random coil conformation transitions

The stability of the chain conformation for macromolecules is remarkably closely related to the solvent polarity, temperature and pH value. It has been revealed that lentinan in aqueous solution undergoes dissociation from a triple helical chain to single random coils under the conditions of $T \geq 130$ °C (T_2) or $w_{DMSO} \geq 0.85$ [90], as shown in Fig. 8b, c, which is called denaturation. The denaturation process occurs in a highly cooperative manner, suggesting that the intra- and intermolecular hydrogen bonds are almost broken simultaneously. The strong alkali environment also shows

an adverse effect on the stability of the triplex structure. The dramatic decreases in weight-average molecular weight M_w, mean square radius of gyration $\langle R_g^2 \rangle$ and intrinsic viscosity $[\eta]$ demonstrate that the helix-coil conformation transition of lentinan occurs in a narrow range of NaOH concentrations between 0.05~0.08 M NaOH [91]. These results indicate that the hydrogen bonding supporting the triple helix structure can be disrupted by solvents with strong polarity or at higher temperatures.

Reformation of the triple helix from the dissociated single chains of lentinan

It has been found that the dissociated lentinan glucan single chains (s-LNT) can be reassembled into the triplex structure (coded as r-LNT) under certain conditions, in which the reconstruction of hydrogen bonding is closely involved [85]. However, the originally matched polymer chains can rarely combine with each other, resulting in the coexistence of complicated products such as worm-like, circular, duplex segment, Y shape-like, crossover species, and so on [92]. This imperfect triple helical structure exerts an attenuated effect on its biological functions. Thus, eliminating structural defects in the regenerated triple helix lentinan appears to be an important subject, particularly in the extraction process using an alkali solution with a high concentration of 1.25 M NaOH. Therefore, the reconstruction process of the triple helix lentinan must be investigated systematically. In our findings, the structural defects can be readily removed during the reconstruction process by modulating the recovery conditions [85]. As shown in Fig. 8d, when a large amount of water was added instantaneously into the lentinan/DMSO solution (RL mode), some structural defects, such as duplex segments, were present in the triple helix; when reconstruction was carried out via dialysis (DL mode) or mimic dialysis (ML mode), water was slowly added into the lentinan/DMSO solution at a uniform rate to avoid the occurrence of a high content of water in the local region, and all random coils with the matched chain size could be well organized into the intact triple helix. Namely, the dissociated single lentinan chains were reassociated into intact triple helices as long as the water fraction slowly increased sufficiently, indicating that the single β-glucan chains have a strong nature to form triple helical structures. These results provide a scientific basis for better understanding the relationship between the high-order structure and physiological function of the reconstructed triple helix lentinan.

Biological functions of lentinan

Antitumor activity

Lentinan is now a commercial polysaccharide used as an adjuvant agent in anticancer chemotherapy, and its outstanding anticancer activity was first identified by Chihara et al. in 1969 [78]. Since then, concerns have focused on its antitumor activities with the goal of unveiling more possibilities against HT-29 tumors, breast cancer, lung cancer and so on [93–96]. In our findings, lentinan has been demonstrated to show a profound inhibition ratio of ~53% against estrogen receptor-positive (ER+) MCF-7 tumor growth in nude mice by suppressing cell proliferation and enhancing apoptosis, possibly via multiple pathways, including phosphatidylinositol 3-kinase/protein kinase B/mammalian target of rapamycin (PI3K/Akt/mTOR), nuclear factor kappa-B (NF-κB), extracellular signal-regulated kinase (ERK), estrogen receptor α (ERα), caspase and tumor suppressor p53-dependent pathways (Fig. 9a) [97]. Lentinan also significantly inhibits H22 tumor growth with an inhibition efficiency of up to 73% without damaging organisms [98]. The relatively low molecular weight with a range of 3.01×10^5~9.18×10^5 and higher stiffness are favorable for the higher antitumor activity than that for molecular weights higher than 1.0×10^6 (Fig. 9b). The notable efficiency was found to be associated with the stronger interactions of the isolated extended triple helical chains with the receptors on the immune cell membrane, directly increasing the secretion of tumor necrosis factor α (TNF-α) and promoting the cell proliferation of peritoneal macrophages, whole spleen cells and lymphocytes [98, 99]. Accumulated evidence also confirms that lentinan inhibits tumor growth and targets tumor sites with oral, intraperitoneal or intratumoral administration of lentinan by upregulating the CD4+ T cell level in lymphoid organs to reverse the impact of tumor burden, as well as altering the tumor microenvironment by promoting CD4+ T cell and neutrophil infiltration into tumor sites or directly recruiting neutrophils from peripheral blood to kill tumors (Fig. 9c) [100]. These results strongly support the antitumor effect of β-glucans regardless of the mode of administration.

Anti-inflammatory activity

Inflammation is an immediate response of tissue toward harmful stimuli or injury. The anti-inflammatory effect of lentinan is mediated through the regulation of various inflammatory cytokines, such as nitric oxide (NO), (TNF-α) and interferon-γ (IFN-γ). [101]. Liu et al. proved that lentinan decreases the expression of proinflammatory cytokines such as interleukin-13 (IL-13) and cluster of differentiation 30 ligand (CD30 L) by inhibiting TLR4 signaling-mediated inflammatory responses and disrupts the intestinal microbial structure, showing potential therapeutic applications in inflammatory bowel disease (IBD) and colitis-associated cancer (CAC) [102]. In our findings, lentinan extracted by sonication not only inhibited the production of TNF-α and NO in lipopolysaccharide (LPS)-

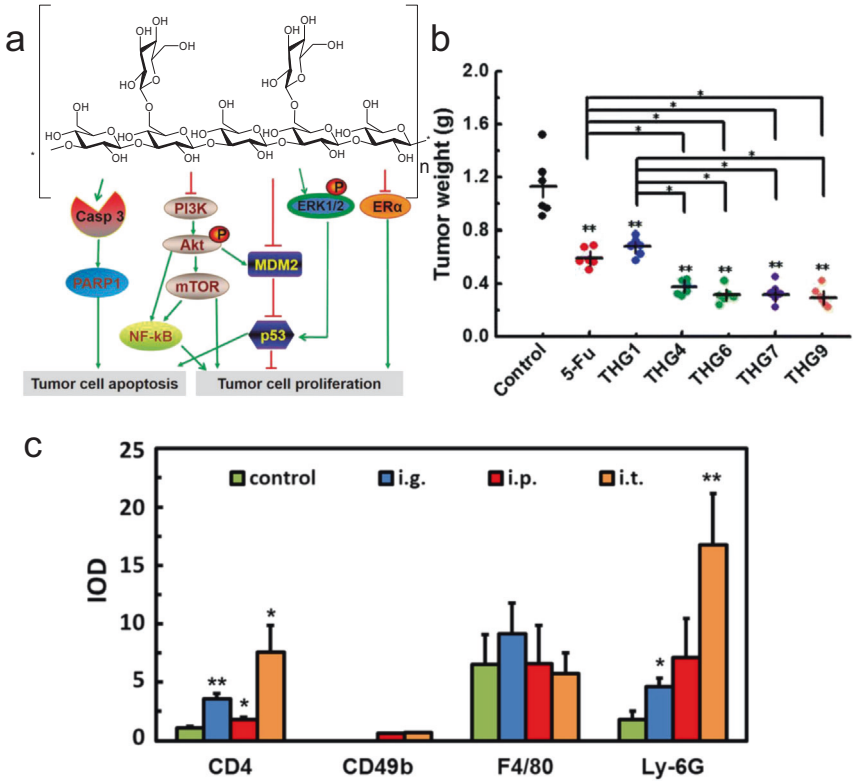

Fig. 9 Antitumor activity and mechanism of lentinan (LNT). Multiple signaling pathways may be involved in LNT-treated ER + MCF-7 breast tumors (**a**) [97]. Copyright © 2017 Impact Journals. The weights of tumors extracted from triple helical glucan (THG)-treated mice bearing H22 tumors. $*p < 0.05$, $**p < 0.01$ vs. control, 5-Fu and THG1. $p < 0.05$ was considered statistically significant (**b**) [98]. Copyright © 2017 The Royal Society of Chemistry. The positive integral optical density (IOD) of surface markers in the immunofluorescence pictures was analyzed by Image-Pro Pro Plus 6.0 software. Data are representative of three independent experiments. $*p < 0.05$, $**p < 0.01$ vs. control. The values of p obtained from statistical analysis represent the difference between the groups. $p < 0.05$ was considered statistically significant (**c**) [100]. Copyright © 2019 Elsevier Ltd

activated macrophage RAW264.7 cells but also decreased the protein expression of inducible nitric oxide synthase (iNOS) and the gene expression of iNOS mRNA and TNF-α mRNA. This striking anti-inflammatory effect may be generated from the pathway partially via the suppression of mitogen-activated protein kinase (MAPK) C-jun N-terminal kinase 1/2 (JNK1/2) and ERK1/2 [80]. Our latest findings indicate that lentinan significantly inhibits intestinal inflammation in dextran sulfate sodium (DSS)-induced colitis in mice (unpublished data). Taken together, both the in vitro and in vivo results demonstrate that lentinan has good anti-inflammatory properties and has potential application in treating inflammatory diseases with greater safety than chemical drugs.

Immunomodulatory activity

The ability to perform significant immunological activities in an innate and adaptive manner for lentinan has long been recognized [103]. Recently, an in vitro immunomodulatory assay demonstrated that lentinan stimulates macrophage phagocytic capacity, improves spleen and thymus indices, promotes lymphocyte proliferation and adjusts the percentages of CD4+ and CD8+ T cells [104]. We have revealed that the immunomodulatory effect of lentinan can also be modulated via the signaling pathway by directly stimulating macrophages. Upstream molecules of MAP kinases, such as ERK1/2 and JNK1/2, are activated through phosphorylation in a time- and concentration-dependent manner. However, the observation of nuclear transcription of NF-κB p65 without any production of proinflammatory mediators (TNF-α and NO) implies that the activation mechanisms of the immune system through modulation by β-glucans are rather complex and depend on many factors that have not yet been fully revealed [105]. The immunomodulatory effects of β-glucans are influenced by differences in their structural characteristics, such as branching frequency, solubility, molecular weight, polymer charge, and conformation in solution. Hence, large challenges still exist, such as determining the structure-function relationships and mechanism of action, which are prerequisites and foundations for their application.

Self-assembly behavior and therapeutic applications of lentinan

The free and reversible conformation transitions between the triple helix and random coils of lentinan are of great importance. On the one hand, biological activities can be well regulated through the dissociation-reconstruction process to maintain the integrity of the triplex structure since single chains of lentinan are detrimental to its biological activities [106, 107]. On the other hand, this unique self-assembly behavior for polymer chains provides more opportunities to fabricate novel nanocomposites with potential applications in cancer therapy and imaging.

Lentinan/nanoparticles

Nanoparticles such as gold nanoparticles (AuNPs), selenium nanoparticles (SeNPs) or carbon nanotubes (CNTs) have been widely used in the biomedical, pharmaceutical and food industries [108–110]. To improve biocompatibility and reduce cytotoxicity, lentinan has been introduced as a soft matrix to accommodate inorganic nanoparticles or fluorescent dyes. Triple helical β-glucan is considered to possess the highest stability for anchoring nanoparticles, possibly because these nanoguests can be easily entrapped into the hydrophobic cavity of the reconstructed triplex structure during the reconstruction process. For example, a novel nanocomposite of lentinan/SeNPs has been prepared by reducing SeO_3^{2-} in the presence of ascorbic acid and s-LNT (shown in Fig. 10a, b). The generated element Se could firmly bind to -OH groups on s-LNT chains through Se-O interactions. Upon the subsequent reconstruction process, the as-formed SeNPs will be wrapped by polymer chains into the cavity of the triple helical structure, thus protecting the Se particle nucleus from further accumulation. Compared to SeNPs/t-LNT, the well-dispersed SeNPs/s-LNT nanocomposites in the solution can remain homogeneous and translucent for a longer period without any precipitates [111]. Moreover, lentinan can serve not only as a capping agent to stabilize nanoparticles but also as a reducing agent in some cases. As illustrated in Fig. 10c, Au^{3+} can be reduced and stabilized by s-LNT, and the as-prepared AuNPs can be converted into nanobelts, spherical nanoparticles, and nanowire morphologies simply by controlling the s-LNT concentration, reaction time and temperature. In the same way, AuNPs can be entrapped and organized into the nanowire in the hydrophobic cavity of reconstructed triple helical lentinan from s-LNT [112].

Benefiting from this feature of reversible conformation transition, other guests, such as silver nanoparticles (AgNPs) and CNTs, have also been immobilized into the lentinan matrix. The as-fabricated AgNP/s-LNT nanoplatform can be used as a color indicator for the formation of polysaccharide aggregates [113], whereas CNT/s-LNT nanocomposites endow CNTs with higher water solubility and cell viability [114]. The water-soluble s-LNT chains can wrap on the surface of hydrophobic CNTs in a helical manner, indicative of a flexible, induced-fit-type size selectivity for lentinan independent of the surface nature of the guest nanoparticles.

In addition, a distinctive self-assembly of triple helical lentinan was reported in our work [115]. It was found that lentinan in water aggregates preferentially along the chain direction to form longer chains, accompanied by side-direction linkage to form branches. With an increase in concentration, the polymer chains of lentinan are arranged in a parallel manner to form dendritic fiber-like aggregates and further intertwine to form fishnets. More interestingly, as shown in Fig. 10d–g, a hydrophobic AIE molecule of tetraphenylethylene (denoted as TPE) can be entrapped into the meshes of lentinan fishnets. Due to the self-assembly of lentinan, the as-prepared lentinan/TPE composite largely enhances the blue fluorescence of TPE in water, exhibiting stable optical properties and good biocompatibility. It is thus promising to carry TPE and its derivatives on lentinan for multifunctional applications in the biomedical field, such as bioimaging and treatment of cancers.

Lentinan/polynucleotide nanocomposites

It has been confirmed that single chains of triple helical β-glucans (e.g., schizophyllan) specifically interact with homopolynucleotides such as poly(C), poly(A), poly(U), poly(T) and poly(dA), thus forming a novel macromolecular complex [116]. This kind of complex consisting of two single chains of the triple helical β-glucan and one chain of polynucleotide can be formed when reformation of the triple helix occurs in the presence of the polynucleotide.

It is generally considered that the combination of hydrophobic and hydrogen-bonding interactions plays an important role in stabilizing the helical structure [40, 117]. In our findings, s-LNT/poly(dA) exhibited higher stability [38], indicating that lentinan can be used as an excellent gene carrier. For example, based on the interaction of s-LNT with poly(dA), a promising strategy for the effective delivery of phosphorothioated antisense oligodeoxyribonucleotide of TNF-α (denoted PS-ATNF-α) targeting intestinal inflammation has been developed [44]. As shown in Fig. 11a, the target of PS-ATNF-α with a poly(dA) tail through a disulfide bond interacts with s-LNT to form a rod-like nanocomposite; PS-ATNF-α is internalized effectively into macrophages with the aid of s-LNT/poly(dA) nanocomposites, downregulating the mRNA expression of the target gene TNF-α and reducing the secretion of TNF-α in the colon with DSS-induced colitis. Furthermore, s-LNT/poly(dA) nanocomposites loaded with PS-ATNF-α can be

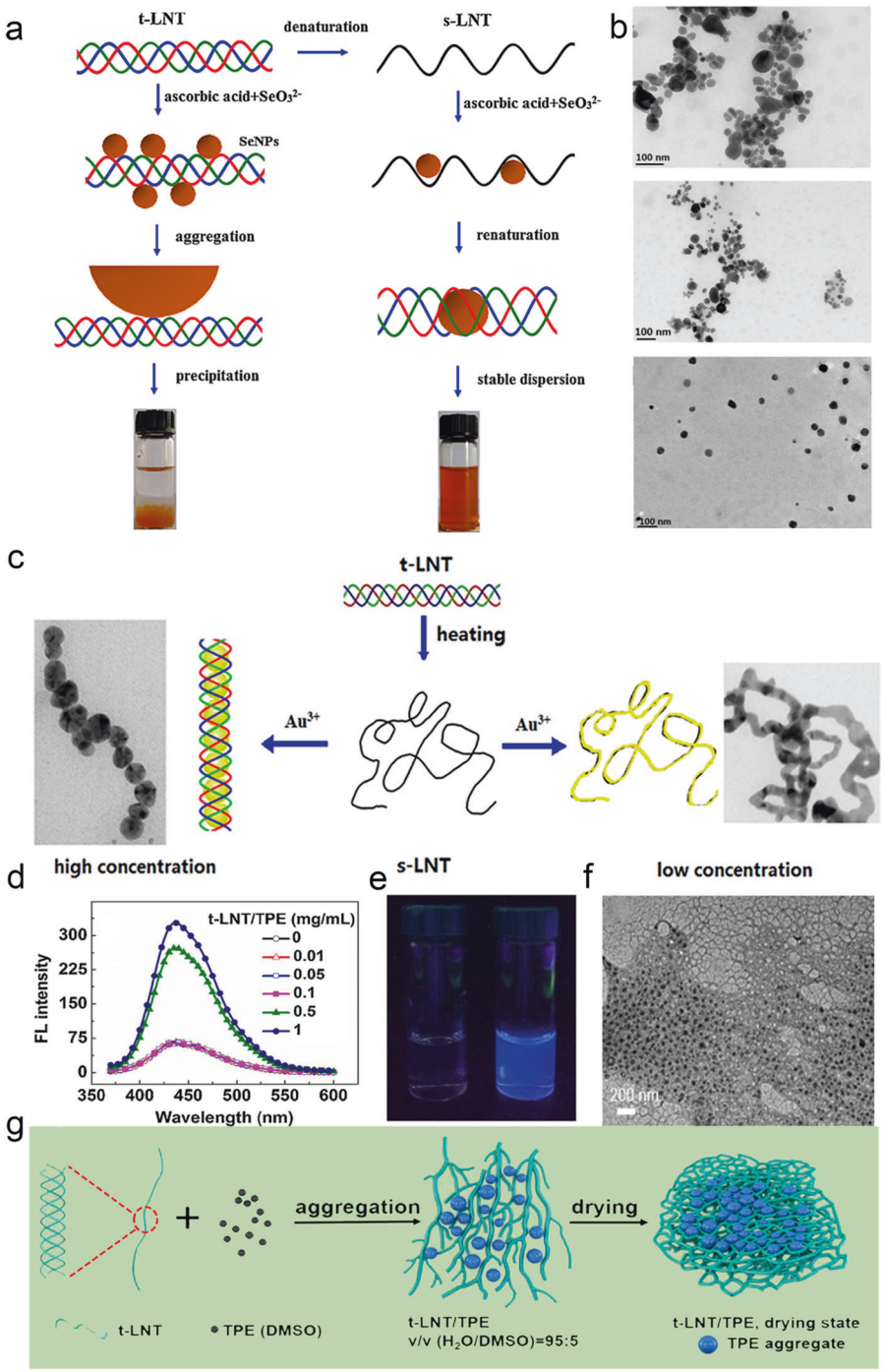

Fig. 10 Formation of lentinan/nanocomposites. Scheme of SeNPs dispersion by s-LNT and t-LNT (**a**). TEM images of selenium nanoparticles in Se/s-LNT-1, Se/s-LNT-2 and Se/s-LNT-3 aqueous solutions (the reaction time was 3 days) (**b**) [111]. Copyright © 2015 Elsevier Ltd. Scheme of the synthesis and dispersion of AuNPs by s-LNT at different concentrations (**c**) [112]. Copyright © 2013, American Chemical Society. Fluorescence emission spectra of t-LNT/TPE with different concentrations of t-LNT in 95% H_2O/DMSO (**d**). Photographs of TPE (left) and t-LNT/TPE (right) in 95% H_2O/DMSO taken under 365 nm UV light illumination with a t-LNT concentration of 0.5 mg/mL (**e**). TEM image of t-LNT/TPE composites with a t-LNT concentration of 0.5 mg/mL (**f**). Scheme of the self-assembly process for t-LNT in water with TPE (**g**) [115]. Copyright © 2017 Elsevier Ltd

orally administered through encapsulation into a hydrogel matrix to inhibit colon colitis progression.

By virtue of the concept of this design, we fabricated a theranostic nanoplatform with biosafety through the specially recognized binding of s-LNT to poly(dA) (Fig. 11b). In the architecture, the s-LNT-Dox conjugates are allowed to combine with poly(dA)-dye into a novel composite of s-LNT-Dox/poly(dA)-dye, with the expectation of simultaneous delivery of Dox and the dye to tumor cells for therapy and bioimaging. Dox and the dye are transported into HeLa cells or tumors with efficient tumor accumulation and bioimaging, dramatically inhibiting tumor growth [118]. Furthermore, we attached a nucleic acid aptamer (AS1411) to the poly(dA) tail and constructed an alternative s-LNT-FITC/poly(dA)-aptamer composite (FITC, fluorescein isothiocyanate) (Fig. 11c) to enhance the targetability. Due to the incorporation of an aptamer, this nanocomposite biomaterial is demonstrated to display enhanced cellular

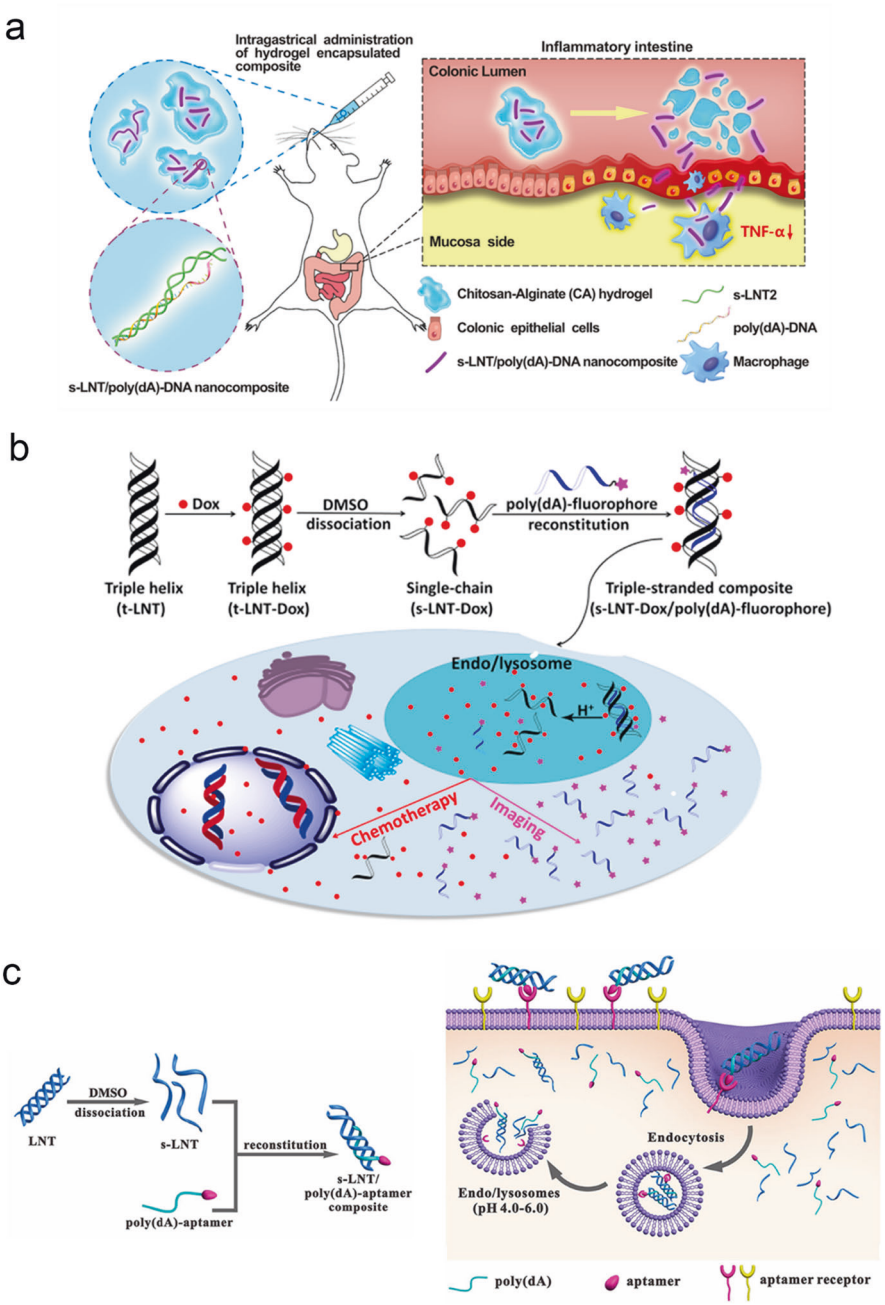

Fig. 11 Schematic diagram of intragastric administration of s-LNT/poly(dA)-DNA nanocomposites encapsulated in the chitosan-alginate (CA) hydrogel and the specific release in the inflammatory intestine to suppress TNF-α production (**a**) [44]. Copyright © 2019 John Wiley and Sons. Schematic illustration of the preparation and intracellular release of s-LNT-Dox/poly(dA)-dye (Dox, doxorubicin hydrochloride) (**b**) [118]. Copyright © 2019, American Chemical Society. Schematic illustration of the fabrication process and the targeted uptake of s-LNT/poly (dA)-aptamer composites (**c**) [119]. Copyright © 2021 Elsevier Ltd

internalization [119]. These results provide more alternative strategies for constructing *β*-glucan-based delivery systems, where various chemotherapy drugs, imaging reagents and functional groups can be introduced to this platform according to the therapeutic requirements, showing great potential in personalized tailored medical therapy.

Yeast *β*-glucan

Yeast is a kind of fungus in the *genus Saccharomyces* and has been used for the fermentation of wine and bread for thousands of years [120]. Commonly, yeast particles present a spherical or columnar shape with a size of ~2–4 μm. The major constituents of the yeast cell wall are polysaccharides, accounting for ~80–90%, such as *β*-(1,3)-glucan, *β*-(1,6)-glucan, mannan and a minor fraction of chitins and proteins [121–123]. In particular, yeast *β*-glucans, as the dominant structural polysaccharide, have been proven to show significant immunomodulatory properties; thus, yeast β-glucans have been approved as novel food ingredients by the European Food Safety Authority [124] and recognized as safe by the US Food and Drug Administration [121].

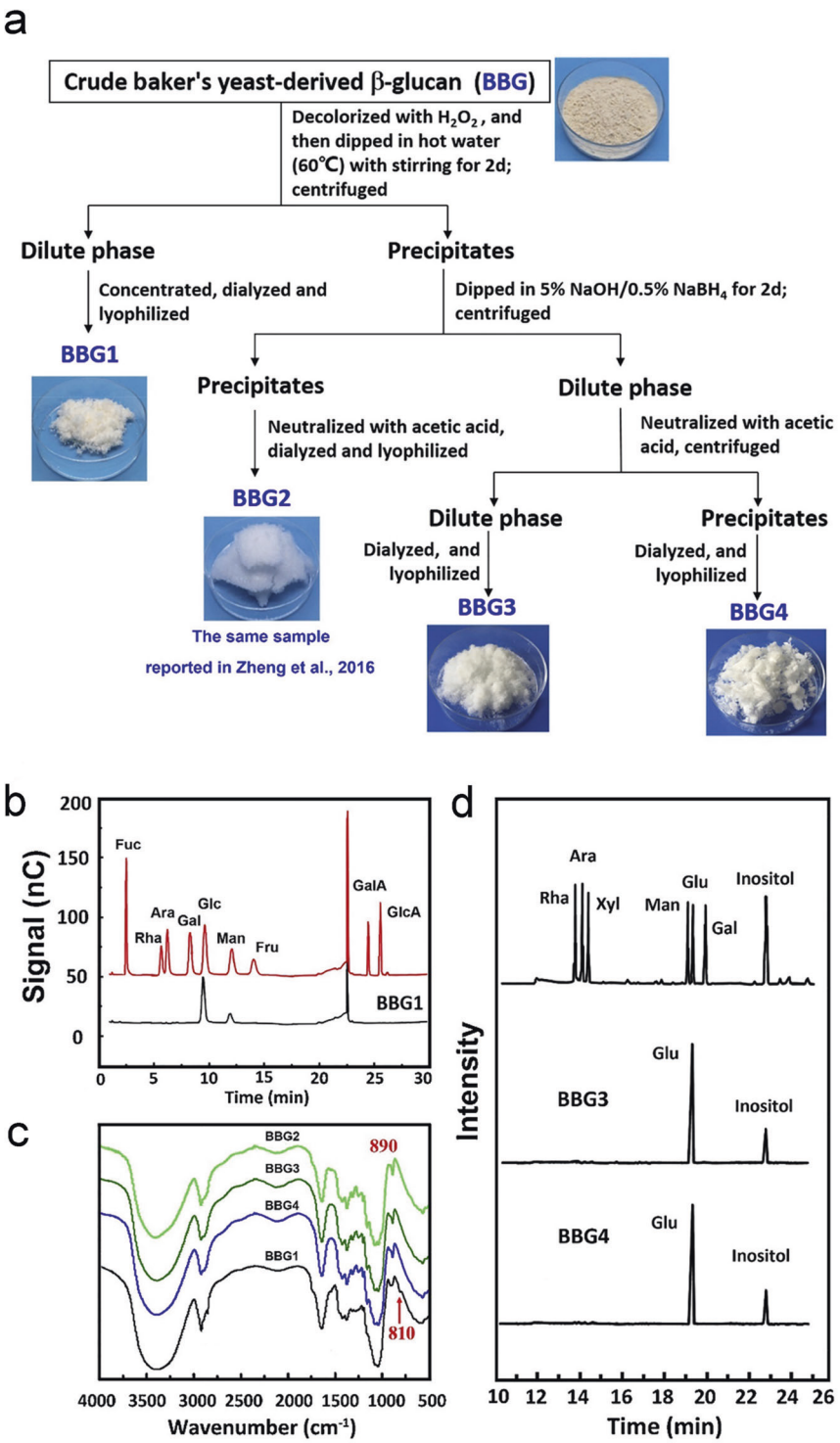

Fig. 12 Purification of the crude BBG (**a**). Structure characterization of BBG1-BBG4 (**b**–**d**). High-performance anion exchange chromatography spectra of monosaccharide standards and BBG1 hydrolysates (**b**). FT-IR spectra of BBG1-BBG4 (**c**); GC spectra of BBG3 and BBG4 (**d**) [125]. Copyright © 2019 Elsevier Ltd

Extraction and chemical structure of yeast β-glucan

Usually, yeast β-glucan with relatively high purity can be obtained with the assistance of chemical extraction technology, which is crucial for clarifying its biological activities and mechanisms. As demonstrated in Fig. 12a, four fractions with different structures are purified from crude yeast β-glucan (denoted as BBG) by hot water and NaOH, which are coded as BBG1, BBG2, BBG3 and BBG4, respectively. Characterization revealed that BBG1 is a composite of highly branched β-(1,6)-glucan linked with mannoprotein, BBG2 displays a linear structure of β-(1,3)-glucan, BBG3 is a β-(1,3)-glucan with a small number of β-(1,6)-branches, and BBG4 is a hybrid consisting of linear

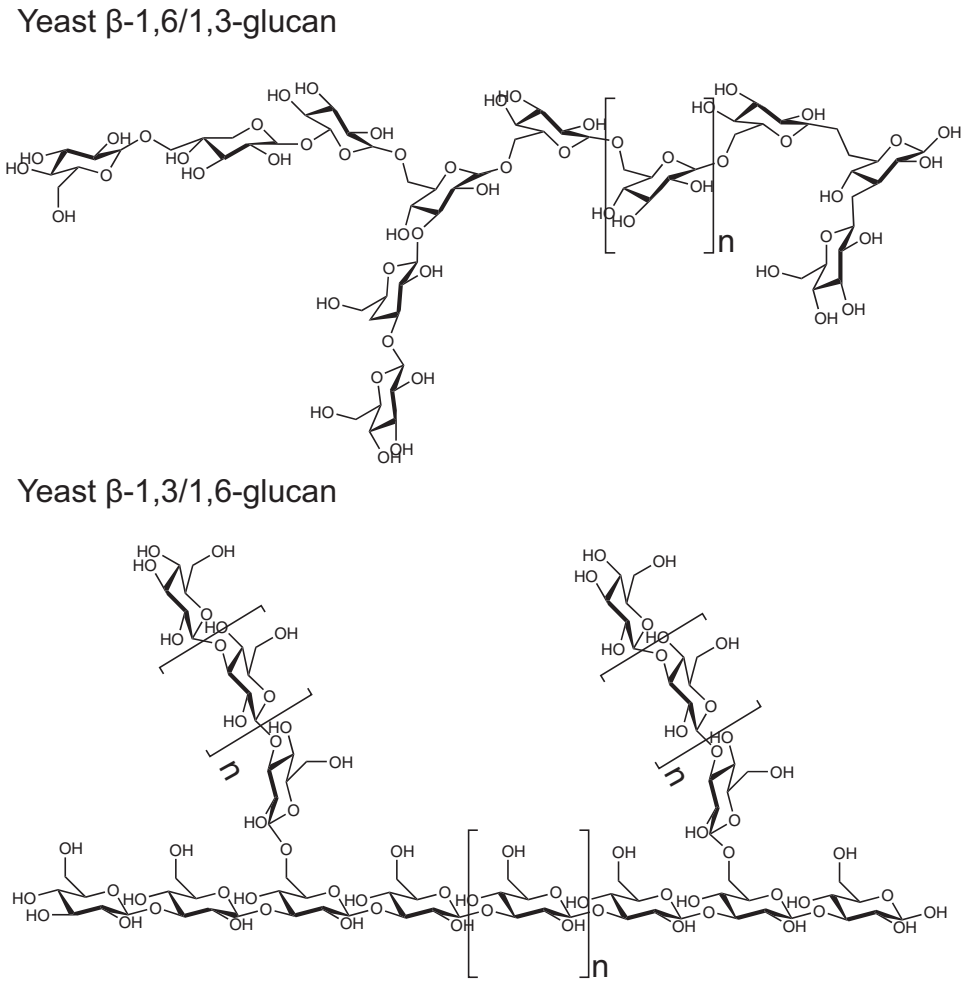

Fig. 13 Structures of *β*-(1,3)-branched *β*-(1,6)-glucan and *β*-(1,6)-branched *β*-(1,3)-glucan from the yeast cell wall [121]. Copyright © 2013 John Wiley and Sons

β-(1,3)-glucan as a major and *β*-(1,6)-branched *β*-(1,3)-glucan as a minor (Fig. 12b–d) [125]. For BBG2 and BBG4, the glucose contents reached 98%. In addition, ultrasonic or enzymatic-assisted extraction is employed to isolate *β*-(1,3)-D-glucan from yeast without any damage to the biological activity of its origin, and the extraction efficiency has been quantified up to 50.5% [126, 127].

After successive alkaline and acidic treatments, branched *β*-(1,3)-D-glucan and *β*-(1,6)-D-glucan account for ~85% and 15% of the total polysaccharides in the yeast cell wall, respectively [128]. Namely, *β*-glucan is the major component.

As indicated in Fig. 13, the two types of glucans present different physical features. *β*-(1,3)-D-glucan with a linear high-molecular-weight chain, along which side chains of *β*-(1,6)-D-glucopyranosyl units that are randomly dispersed, is alkali-insoluble, while the shorter polysaccharide consisting of *β*-(1,6)-D-glucan backbones, which may act as a flexible glue due to their ability to covalently cross-link to *β*-(1,3)-D-glucan, chitin and mannoprotein, is alkali-soluble [129, 130]. The structural features of *β*-glucan from yeast are shown in Table 1.

Chain conformation

A major obstacle to identifying the chain conformation is its poor solubility in aqueous media. Although disputes exist, *β*-glucan is suggested to adopt both a single helix and triple helix conformation, which was confirmed by X-ray diffraction and Magic-Angle Spinning ^{13}C-NMR [131, 132]. More evidence has been obtained from the molecular weight analysis of a water-insoluble yeast-derived *β*-glucan by organic-phase size-exclusion chromatography, where the water-insoluble yeast-derived *β*-glucan was converted into water-soluble pharmaceutical-grade glucan phosphate without destruction of its native structure [133].

Interestingly, after intensive treatment with a combination of alkaline, acidic solution and organic solvent, the yeast cells exhibit a special morphology by partially removing the soluble components from the inner core. In our findings, the resultant particles maintained the shape of yeast cells and displayed a uniform size of 2~4 μm with a porous and hollow structure (Fig. 14). The particle shell primarily composed of *β*-glucan (>90%) facilitates receptor-mediated phagocytic cell uptake [134]. Meanwhile, the

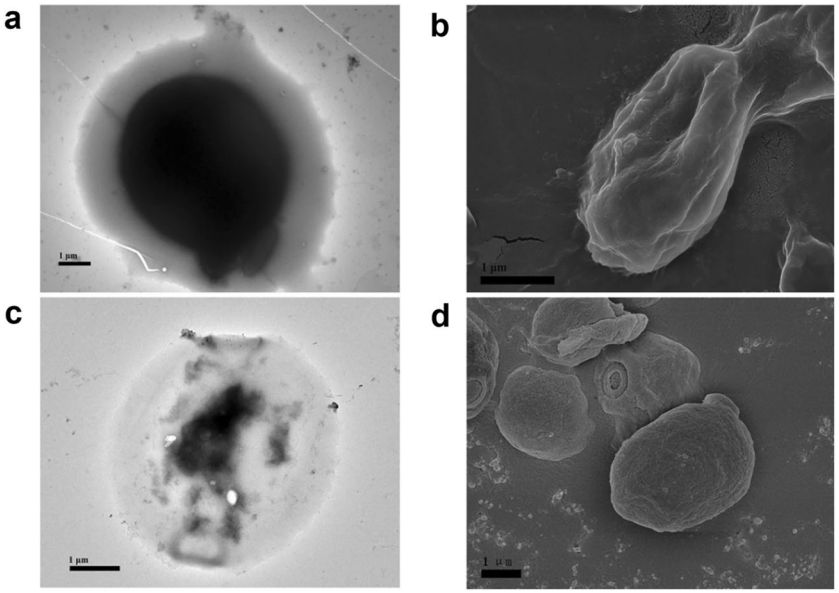

Fig. 14 TEM image of intact yeast (**a**). SEM image of intact yeast (**b**). TEM image of yeast glucan particle (YGP) (50 mg/mL) (**c**). SEM image of YGP (**d**)

hollow cavity of the particles allows for adsorption and encapsulation of payload molecules. Therefore, the yeast β-glucan-derived carrier can be considered an ideal candidate for targeting drug delivery with higher internalization efficiency [135].

Biological activity of yeast β-glucan

Yeast-derived β-glucans as immunomodulatory agents may activate the host immune response and thereby promote resistance to infections or cancer development/progression [121, 136]. These insoluble particles can be phagocytosed by dendritic cells and macrophages via the recognition of dectin-1, complement receptor (CR3) or TLR-2/6 receptor, leading to the T-cell response and cytokine release [121, 137, 138]. Moreover, yeast β-glucans exhibit high efficiency in anti-inflammatory and hypoglycemic activities.

Immunomodulatory activity

The immunomodulatory effects of yeast β-glucans are demonstrated to be mediated primarily through their recognition by specific receptors. These so-called pattern recognition receptors (PRRs) play important roles in host defense and present specific opportunities for clinical modulation of the host immune response. Of these, dectin-1 is the most commonly studied β-glucan receptor, which is a type II transmembrane protein C-type lectin receptor expressed on monocytes, macrophages, neutrophils and dendritic cells (DCs) [139]. When dectin-1 is bound to β-glucan, such as zymosan, it induces the production of various cytokines and chemokines, including TNF-α, CXC-chemokine ligand 2, IL-2, IL-10 and IL-12, and gives rise to the respiratory burst through phagocytosis and possibly endocytosis [140]. In most cases, this intracellular signaling mainly depends on the cytoplasmic immunoreceptor tyrosine-based activation motif (ITAM) as well as the activation of a PI3K/Akt pathway [141, 142]. In addition, the immunomodulatory effects of β-glucans can be modulated by means of oral administration. β-glucans can be phagocytosed by intestinal epithelial cells or pinocytic microfold cells (M-cells) and further transported from the intestinal lumen to immune cells within Peyer's patches [121, 137]. Following exposure to β-glucans, gastrointestinal macrophages might migrate through the bloodstream toward the lymph system, ultimately exerting their immunomodulatory functions [143].

Anti-inflammatory activity

Anomalous and perpetual inflammation may cause various pathophysiological conditions, including hepatitis, atherosclerosis and cancer [144]. Yeast β-glucan can interact with cells of the innate immune system to trigger an adaptive anti-inflammatory response.

In our findings, yeast β-glucan suppresses LPS-induced NO production by 35–70% independent of dectin-1, possibly by suppressing iNOS expression and downregulating the TLR4/JNK and TLR2 pathways. Meanwhile, the production of several cytokines, including interleukin IL-1α, IL-1ra, and IL-27, is attenuated by treatment with yeast β-glucan particles, showing potential as a powerful inhibitor of inflammatory stimuli [145]. Recently, we also revealed that Baker's yeast β-glucans (BBGs) display anti-inflammatory effects in intestinal inflammation therapy. As indicated in Fig. 15a, b, the disease index (DAI), colon

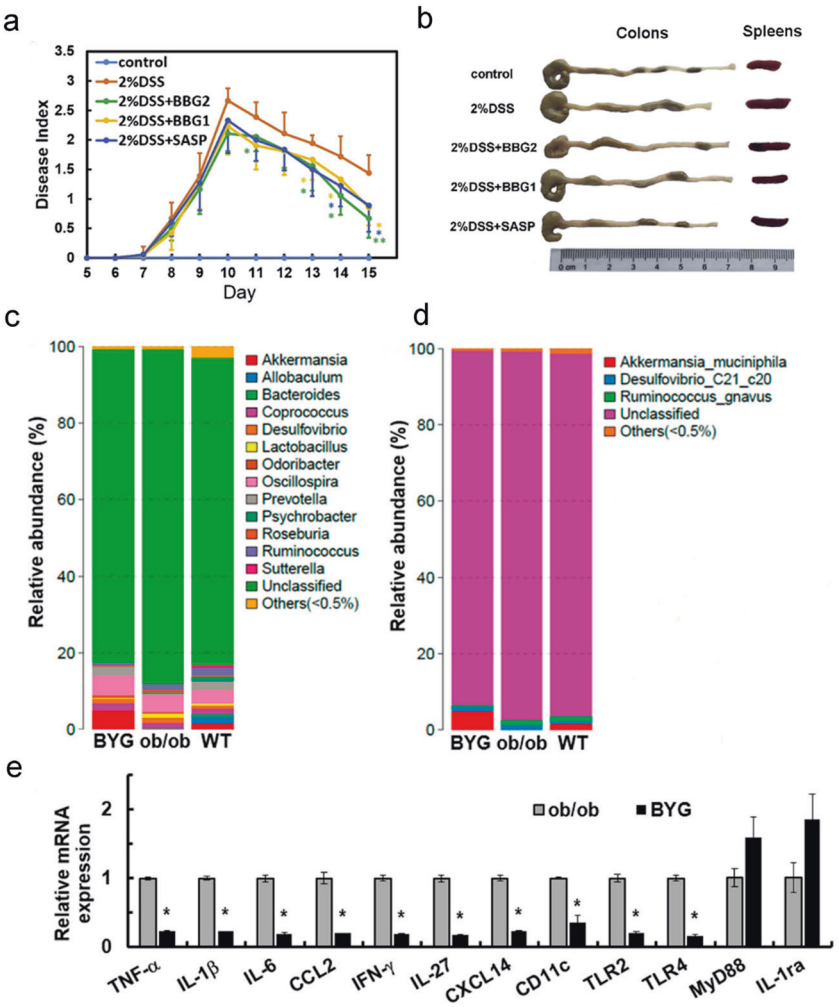

Fig. 15 Anti-inflammation of yeast β-glucan. Yeast *β*-glucan BBG2 reduces inflammation in colitis mice, as indicated by the disease index (DAI) score determined by combining scores of body weight loss, stool consistency and stool bleeding. $*p < 0.05$, $**p < 0.01$ vs. 2% DSS group. $p < 0.05$ was considered statistically significant (**a**). Images of colons and spleens extracted from mice with colitis after treatment for 15 days (**b**) [125]. Copyright © 2019 Elsevier Ltd. Yeast *β*-glucan (BYG) alters the gut microbiota and inhibits intestinal inflammation in ob/ob mice (**c**–**e**). Bacterial community distribution identified at the phylum (**c**) and genus (**d**) levels; effects of BYG on the mRNA levels of pro- and anti-inflammatory cytokines in the intestines of ob/ob mice. $*p < 0.05$ vs. control group (ob/ob mice). All the p values above obtained from statistical analysis represent the difference between the groups. $p < 0.05$ was considered statistically significant (**e**) [146]. Copyright © 2018, American Chemical Society

lengths and spleen sizes of mice, which reflect the severity of clinical symptoms, were obviously lowered by yeast *β*-glucan (BBG2) compared with those in the DSS-induced model group, suggesting that orally administered yeast *β*-glucan reduces the clinical symptoms and promotes recovery of colitis mice. This occurrence seems to be ascribed to the weakness of the pro-inflammatory mediators of IL-6, iNOS and IL-1β at the protein and/or mRNA levels, as well as the reduction of colonic mucosal damage and macrophage infiltration in DSS-induced colitis mice [125].

Chronic inflammation widely exists in visceral adipose tissues (VATs), especially for patients with long-term metabolic pathogenesis of obesity, insulin resistance and type-2 diabetes. The dramatic inhibitory effect of yeast *β*-glucan on chronic inflammation was also observed in our work. With oral administration, yeast *β*-glucans improve the microenvironment in adipose tissues and suppress chronic inflammation by stimulating immune responses. Yeast *β*-glucan (BYG) decreases the pro- and anti-inflammatory cytokines TNF-α, IL-6, IL-1β, IL-10 and IL-1ra (Fig. 15e) and increases the anti-inflammatory factor Azgp1 at the protein and/or mRNA levels. Furthermore, BYG increased the gut microbiota proportion of *Akkermansia* from 0.07% to 4.85% and improved the microenvironment of VATs by decreasing fibrosis and angiogenesis (Fig. 15c, d). All of these benefits suggest that yeast *β*-glucans have significant anti-inflammatory activity in diabetic hosts and can be used as a food component and/or therapeutic agent for diabetes [146].

Antitumor activity

Yeast-derived *β*-glucan can exert its antitumor effects in a variety of ways. For example, yeast *β*-glucan particles decrease the accumulation of polymorphonuclear myeloid-derived suppressor cells (MDSCs) in the tumor microenvironment through the induction of respiratory burst and apoptosis. MDSCs are a heterogeneous population of immature myeloid cells that contribute to tumor escape from immunological attack; thus, after treatment with yeast *β*-glucan, the tumor weight and splenomegaly in tumor-bearing mice were significantly reduced. Meanwhile, yeast

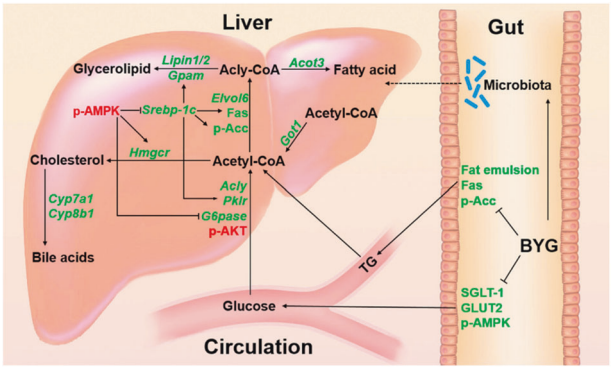

Fig. 16 Proposed mechanism by which BYGlc ameliorates glucose and lipid homeostasis in ob/ob mice. Orally administered BYGlc suppresses intestinal SGLT-1, glucose transporter 2 (GLUT2), and fat emulsification to decrease intestinal glucose and lipid absorption. The changed microbiota is attributable to the ameliorated glucose/lipid homeostasis in the liver, indicated by the upregulated protein expression of phosphorylated AKT (p-AKT) and phosphorylated adenosine monophosphate activated protein kinase (p-AMPK) and restrained gene expression of rate-determining enzymes in gluconeogenesis (G6pase and Got1), fatty acid biosynthesis (*Acly, Acc, Fas, Elovl6*, and *Acot3*), glycerolipid synthesis (*Gpam* and *Lipin2/2*), and cholesterol and bile acid metabolism (*Hmgcr, Cyp7a1*, and *Cyp8b1*) pathways [153]. Copyright © 2017, American Chemical Society

β-glucan-treated monocytic MDSCs (M-MDSCs) can be induced to differentiate into potent antigen-presenting cells (APCs) via the ERK1/2 phosphorylation pathway, leading to a decrease in tumor burden [147]. Qi et al. revealed that yeast β-glucan improves its antitumor responses by directly abrogating tumor-educated dendritic cell-associated immune suppression and promoting Th1 differentiation and cytotoxic T lymphocyte priming [148]. Furthermore, yeast-derived β-glucan is verified to delay tumor growth by converting polarized alternatively activated macrophages or immunosuppressive tumor-associated macrophages (TAMs) into a classically activated phenotype with potent immune-stimulating activity. This process is associated with macrophage metabolic reprogramming and can be mediated via the dectin-1-induced spleen tyrosine kinase-Card9-Erk pathway. These findings have established a new paradigm for macrophage polarization and immunosuppressive TAM conversion and shed light on the mode of action of β-glucan treatment in cancer [149].

Hypoglycemic activity

It has long been known that consumption of a diet high in crude yeast β-glucan particles can prevent insulin resistance and balance blood glucose, showing powerful ability in the treatment of obesity and diabetes [150, 151]. However, the uncertainty of diverse ingredients and chemical structures in yeast β-glucan usually leads to chaotic and inconsistent bioactivities and mechanisms. In our work, the hypoglycemic activity of purified Baker's yeast β-glucan with a defined chemical structure was tentatively elucidated. Oral administration of high-purity β-glucan (BYGlc) has a beneficial effect on metabolic disorders in diabetic mice. BYGlc can promote hepatic glycogen synthesis and decrease hepatic lipid accumulation through the insulin receptor substrate (IRS)/Akt insulin signaling pathway. More importantly, BYGlc inhibits the expression of glucose transporter sodium-glucose transporter-1 (SGLT-1) and alters the population of gut microbiota, thus resulting in a decrease in blood glucose and alleviating chronic inflammation [152]. Further research revealed that BYGlc downregulates gluconeogenesis-associated gene (*G6pase* and *Got1*) levels and reduces the gene expression of fatty acid biosynthesis (*Acly, Acc, Fas, Elovl6*, and *Acot3*), glycerolipid synthesis (*Gpam* and *Lipin2/2*) and cholesterol synthesis (*Hmgcr, Cyp7a1*, and *Cyp8b1*) (Fig. 16). Overall, BYGlc exerts its hypoglycemic activity by reducing liver glucose output, lowering blood sugar and inhibiting the accumulation of fat in the liver [153].

Potential therapeutic applications

Yeast β-glucan particles with hollow cavities can target phagocytic cells through M cell-mediated endocytosis, making them excellent candidates for drug delivery as well as bioimaging agents [136]. In addition, they display advantages such as convenience, good safety profile, easy control and greater patient compliance. Hence, yeast-associated nanoparticle-based microencapsulation offers a promising strategy for the treatment of various medical conditions.

Drug delivery

Drugs can usually be encapsulated into yeast β-glucan particles with cavities by utilizing precipitation, lyophilization or reversed-phase evaporation methods depending on the nature of the drug molecules [134, 154, 155]. Following sealing treatment to trap the guests into the cavity, the as-prepared nanoplatform can successfully deliver the payloads to targeted sites. For example, a water-insoluble drug of rifampicin used in tuberculosis treatment has been efficiently loaded into yeast β-glucan particles with the help of alginate or chitosan hydrogels [134]. The resulting formulation exhibits slow and continuous release behavior for 24~72 h and reduces intracellular tuberculosis levels in infected bone marrow-derived macrophages. Small water-soluble compounds can also be encapsulated into the hydrophobic cavity through the reversed-phase evaporation method [154]. Depending on the characteristics of the liposomes entrapped in the particles, this construct may act

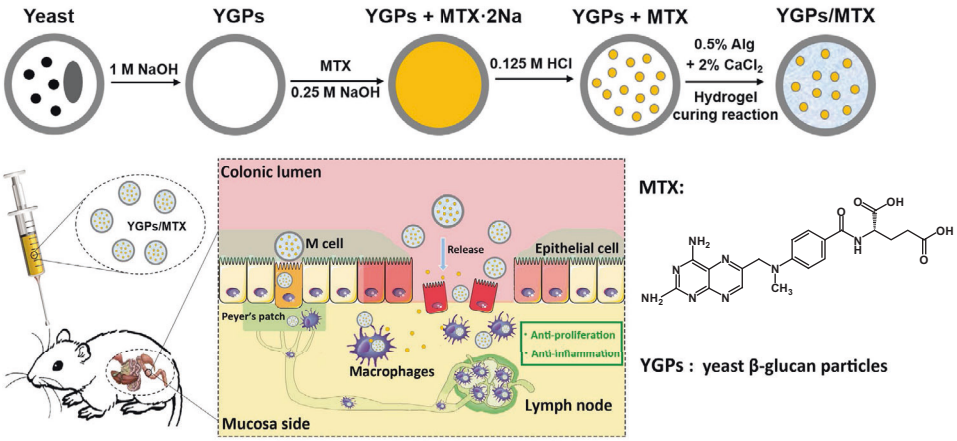

Fig. 17 Scheme of the strategy using yeast glucan particles (YGPs) as carriers to deliver MTX to the inflamed colon. MTX is loaded into hollow YGPs through reprecipitation followed by gelation to obtain YGPs/MTX; YGPs/MTX are internalized by macrophages through dectin-1 and CR3 receptors mediated after oral administration by gavage and target the intestinal inflammation site [155]. Copyright © 2020 John Wiley and Sons

as a biocompatible carrier to deliver and release in a triggerable way.

Benefitting from the native biological activities of anti-inflammatory and antitumor agents, yeast β-glucan particles can synergize with small molecule drugs to exert better therapeutic effects. For example, a targeted oral delivery system of yeast β-glucan particles carrying the anti-inflammatory drug methotrexate (MTX) has been developed, as shown in Fig. 17. MTX can be loaded into yeast glucan particles (YGPs) through reprecipitation with a high encapsulation efficiency of up to 85%. Following immobilization of the alginate hydrogel, the obtained composites can be internalized into RAW264.7 macrophage cells through dectin-1 and CR3 receptors. Furthermore, this microcapsule can suppress the proliferation of macrophage cells efficiently, leading to downregulation of proinflammatory cytokines induced by LPS. Accumulation of the nanocomposite in the inflammation site of colitis mice enables it to target the inflammatory site, significantly improving the uptake of MTX and reducing the cytotoxicity of MTX [155].

Gene delivery

Based on the vesicle structure, the encapsulation of anionic plasmid DNA or siRNA into yeast β-glucan particles has also been achieved via layer-by-layer assembly induced by electrostatic interactions [156, 157]. By creating a positive core of tRNA/polyethylenimine (PEI), the target gene sections can be firmly bound into the cavity of yeast β-glucan particles for further application of transfection. For example, the as-formed formulations containing plasmid gWizGFP effectively transferred the genes into NIH3T3-D1 cells even with a rather low dose value of 125 ng of DNA/5×10^5 cells, whereas the transfection efficiency of DNA/PEI nanocomplexes that were not entrapped inside yeast β-glucan particles was negligible [156]. In the same way, engineered β-glucan-encapsulated siRNA particles can be taken as efficient oral delivery vehicles to attenuate systemic inflammation by targeting macrophage mitogen-activated protein kinase kinase kinase kinase-4 (MAP4K4) [157]. The results indicate that oral gavage of mice with these microcapsules containing as little as 20 μg/kg siRNA can direct against TNF-α and silence messenger RNA in macrophages recovered from the peritoneum, spleen, liver and lung. This high potency is considered to be related to the protection of siRNA against nuclease degradation, low nonspecific binding of these formulations to the gut, and high uptake efficiency by phagocytic cells in the gut-associated lymphatic tissue.

Vaccine delivery

The development of yeast β-glucan particle-derived microcarriers has provided a promising strategy for vaccination by applying safe, biodegradable and nonreplicating antigen delivery systems. Yeast β-glucan can be internalized into human intestinal epithelial cell lines and elicit cellular and humoral immune responses without exerting negative effects on cell viability. Hence, yeast β-glucan vehicles can serve as an oral antigen delivery system. Smet et al. showed that β-glucan particles are able to deliver ovalbumin (OVA) *via* an oral route, allowing efficient antigen presentation alongside adaptive immune activation, resulting in a Th17-biased response and the production of OVA-specific IgA, secretory IgA and secretory component antibodies [17]. Hong et al. also reported that aluminum salt can be encapsulated into yeast β-glucan vehicles as an oral vaccine adjuvant for potential utilization in the treatment of cancer and infectious diseases. These hybrid particles can be highly specifically targeted to APCs and strongly activate dendritic cell (DC) maturation and cytokine secretion. Further studies indicate that this particulate system can elicit a strong Th1-biased immune response and extremely high antibody titer and cause marked prophylactic and therapeutic effects against tumors, showing an excellent ability to stimulate

humoral and cellular immune responses at the same time [158].

Bioimaging

Bioimaging is usually used in disease diagnosis. Diverse charged nanoprobes, including quantum dots (QDs), iron oxide nanoparticles (IONPs), and assembled organic fluorescent nanoparticles, can be effectively loaded into yeast capsules (YCs) through electrostatic force-driven spontaneous deposition, resulting in different diagnostic assemblies. YCs containing either nanoprobes or nanotherapies may be rapidly endocytosed by macrophages and maintained in cells for a relatively long period of time. The nanoparticles packaged in YCs are first transcytosed by M cells and sequentially endocytosed by macrophages, then transported to neighboring lymphoid tissues, and finally delivered to remote diseased sites of inflammation or tumors in mice or rats through the natural route of macrophage activation, recruitment, and deployment, affording remarkably improved efficacies for the treatment of multiple diseases associated with inflammation. A system with the capability to precisely and conveniently deliver nanoparticles through oral administration opens a new avenue for the diagnosis and treatment of many diseases [36].

Based on the above, yeast β-glucan particles offer a promising platform for oral delivery of payloads to distant sites. Taking advantage of yeast β-glucan particles, including high loading capacity, oral bioavailability, β-glucan receptors targeting macrophages and dendritic cells, cell trafficking to the reticuloendothelial system and sites of pathology, these microcapsules are expected to serve as a bioinspired delivery system for more therapeutic cargos. Moreover, the exploration of genetically engineered yeast is needed due to the high survival rate in the digestive tract.

Conclusions and future perspectives

Natural polysaccharides, particularly β-glucans, have attracted much attention and have been widely applied in the field of biomedicine due to their good biocompatibility and various bioactivities. In this review, the chemical structure, chain conformation, biological activity, and therapeutic applications of three representative β-glucans of AF1 from AAJ, lentinan from *Lentinus edodes* and yeast β-glucan were summarized.

Studies on the structures and chain conformation have confirmed that AF1, lentinan and yeast β-glucan are all triple helix β-glucans containing a backbone of linear β-(1,3)-glucan with or without β-(1,6)-branches. Of these, triple-helix AF1 can self-assemble in parallel into nanotubes or nanofibers owing to its stiff conformation, and the hydrophobic cavity of AF1 nanotubes can be applied as a one-dimensional host for many target guests, such as DNA, nanoparticles and small functional molecules. Similar to a water-soluble triple helix β-glucan, the conformational transition between the triple helix and random coil of lentinan is another crucial issue. The random coil can be well organized into an intact triple helix by modulating recovery conditions, and nanoparticles can be easily entrapped into the triple helix cavity during the dissociation-reconstruction process. In particular, the single chains of lentinan and homopolynucleotides can be associated into a heterotriple helix, which can be used as a gene carrier. For yeast β-glucan particles, the inherent hollow and porous vesicle structure makes them quite suitable as drug carriers. It is worth mentioning that triple helix β-glucans possess various bioactivities, such as antitumor, anti-inflammatory, and antidiabetic activities. The underlying molecular mechanism has been proposed: the triple helix β-glucan can be specifically recognized by receptors on the immune cell surface, such as dectin-1 or Toll-like receptors, to activate the host's immune response. Currently, several health products derived from these natural polysaccharides have been employed in clinical practice. The low cytotoxicity, various activities and targetability of β-glucans endow them with great potential in the food and medicine fields as functional food, drugs, and biomedical materials.

In view of the abovementioned findings, although pharmaceutical preparations derived from natural polysaccharides exhibit excellent biological activities and have been applied clinically, more structural information and clinical trials are still needed to search for new functions and establish structure-function relationships. In particular, little information on the higher ordered structure of polysaccharides is known, and they may play key roles in interactions with cells. We believe that there are many new functions undisclosed for polysaccharides, and efforts have to be made to clarify them. In addition, receptors that can specifically recognize these β-glucans have only been discovered on the surface of immune cells until now; however, the interactions between cancer cells and polysaccharides, especially potential receptors on cancer cells, are poorly understood, which is a challenging subject and is worth investigating.

In summary, natural β-glucans with triple helices from *Auricularia auricula*, *Lentinus edodes* and yeast are potential health products with good biocompatibility and promising application prospects. Research and development on β-glucans have great significance in the fields of both food and biomedicine.

Acknowledgements This work was financially supported by the National Natural Science Foundation of China (22075213, 21875167, and 21574102), National Key R&D Program (2016YFD0400202),

National Natural Science Foundation of China (51603195) and Key R&D Plan of Hubei Province (2020BCA079).

Compliance with ethical standards

Conflict of interest The authors declare no competing interests.

Publisher's note Springer Nature remains neutral with regard to jurisdictional claims in published maps and institutional affiliations.

References

1. Faggio C, Pagano M, Dottore A, Genovese G, Morabito M. Evaluation of anticoagulant activity of two algal polysaccharides. Nat Prod Res. 2016;30:1934–7.
2. Yu Y, Shen M, Song Q, Xie J. Biological activities and pharmaceutical applications of polysaccharide from natural resources: a review. Carbohydr Polym. 2018;183:91–101.
3. Peng M, Yi Y, Zhang T, Ding Y, Le J. Stereoisomers of saponins in Panax notoginseng (Sanqi): a review. Front Pharm. 2018;9:188.
4. Li Y, Wang X, Ma X, Liu C, Wu J, Sun C. Natural polysaccharides and their derivates: a promising natural adjuvant for tumor immunotherapy. Front Pharm. 2021;12:679.
5. Hou C, Chen L, Yang L, Ji X. An insight into anti-inflammatory effects of natural polysaccharides. Int J Biol Macromol. 2020;153:248–55.
6. Wang P, Zhao S, Yang B, Wang Q, Kuang H. Anti-diabetic polysaccharides from natural sources: a review. Carbohydr Polym. 2016;148:86–97.
7. Torres FG, Troncoso OP, Pisani A, Gatto F, Bardi G. Natural polysaccharide nanomaterials: an overview of their immunological properties. Int J Mol Sci. 2019;20:5092.
8. Werz DB, Seeberger PH. Carbohydrates as the next frontier in pharmaceutical research. Chem Eur J. 2005;11:3194–206.
9. Meng Y, Zou S, Jiang M, Xu X, Tang B, Zhang L. Dendritic nanotubes self-assembled from stiff polysaccharides as drug and probe carriers. J Mater Chem B. 2017;5:2616–24.
10. Wu C, Wang X, Wang J, Zhang Z, Wang Z, Wang Y, et al. Tile-based self-assembly of a triple-helical polysaccharide into cell wall-like mesoporous nanocapsules. Nanoscal 2017;9:9938–45.
11. Liu Q, Duan B, Xu X, Zhang L. Progress in rigid polysaccharide-based nanocomposites with therapeutic functions. J Mater Chem B. 2017;5:5690–713.
12. Zhang R, Edgar KJ. Properties, chemistry, and applications of the bioactive polysaccharide curdlan. Biomacromolecules. 2014;15:1079–96.
13. Kim HS, Park KH, Lee HK, Kim JS, Kim YG, Lee JH, et al. Curdlan activates dendritic cells through dectin-1 and toll-like receptor 4 signaling. Int Immunopharmacol. 2016;39:71–8.
14. Zhong K, Liu L, Tong L, Zhong X, Wang Q, Zhou S. Rheological properties and antitumor activity of schizophyllan produced with solid-state fermentation. Int J Biol Macromol. 2013;62:13–7.
15. Viñarta SC, Delgado OD, Figueroa LIC, Fariña JI. Effects of thermal, alkaline and ultrasonc treatments on scleroglucan stability and flow behavior. Carbohydr Polym. 2013;94:496–50.
16. Zhang L, Zhang X, Zhou Q, Zhang P, Zhang M, Li X. Triple helix of β-D-glucan from Lentinus edodes in 0.5 M NaCl aqueous solution characterized by light scattering. Polym J. 2001;33:317–21.
17. De Smet R, Demoor T, Verschuere S, Dullaers M, Ostroff GR, Leclercq G, et al. β-Glucan microparticles are good candidates for mucosal antigen delivery in oral vaccination. J Control Rel. 2013;172:671–78.
18. Zhong K, Tong L, Liu L, Zhou X, Liu X, Zhang Q, Zhou S. Immunoregulatory and antitumor activity of schizophyllan under ultrasonic treatment. Int J Biol Macromol. 2015;80:302–8.
19. Farina J, Sineriz F, Molina O, Perotti N. Isolation and physicochemical characterization of soluble scleroglucan from Sclerotium rolfsii. rheological properties, molecular weight and conformational characteristics. Carbohydr Polym. 2001;44:41–50.
20. Xu X, Zhang X, Zhang L, Wu C. Collapse and association of denatured lentinan in water/dimethlysulfoxide solutions. Biomacromolecules. 2004;5:1893–8.
21. Zhang Y, Xu X, Xu J, Zhang L. Dynamic viscoelastic behavior of triple helical lentinan in water: effects of concentration and molecular weight. Polymer. 2007;48:6681–90.
22. Miyoshi K, Uezu K, Sakurai K, Shinkai S. Proposal of a new hydrogen-bonding form to maintain curdlan triple helix. Chem Biodivers. 2004;1:916–24.
23. Takeda H, Yasuoka N, Kasai N, Tokayu H. X-ray structural studies of (1→3)-β-D-glucan (curdlan). Polym J. 1978;10:365–8.
24. Chan GC, Chan WK, Sze DM. The effects of β-glucan on human immune and cancer cells. J Hematol Oncol. 2009;2:25.
25. Han B, Baruah K, Cox E, Vanrompay D, Bossier P. Structure-functional activity relationship of β-glucans from the perspective of immunomodulation: a mini-review. Front Immunol. 2020;11:658.
26. Bashir K, Choi J. Clinical and physiological perspectives of β-glucans: the past, present, and future. Int J Mol Sci. 2017;18:1906.
27. Kim H, Hong J, Kim Y, Han S. Stimulatory effect of β-glucans on immune cells. Immune Netw. 2011;11:191–5.
28. Okamura K, Suzuki M, Chihara T, Fujiwara A, Fukuda T, Goto S, et al. Clinical evaluation of schizophyllan combined with irradiation in patients with cervical cancer: a randomized controlled study. Cancer. 1986;58:865–72.
29. Yang P, Liang M, Zhang Y, Shen B. Clinical application of a combination therapy of lentinan, multi-electrode RFA and TACE in HCC. Adv Ther. 2008;25:787–94.
30. Bae AH, Numata M, Hasegawa T, Li C, Kaneko K, Sakurai K, Shinkai S. 1D arrangement of Au nanoparticles by the helical structure of schizophyllan: a unique encounter of a natural product with inorganic compounds. Angew Chem Int Ed. 2005;44:2030–3.
31. Numata M, Tamesue S, Fujisawa T, Sakurai K, Shinkai S. Beta-1,3-glucan polysaccharide (schizophyllan) acting as a one-dimensional host for creating supramolecular dye assemblies. Org Lett. 2006;8:5533–6.
32. Numata M, Asai M, Kaneko K, Bae AH, Hasegawa T, Sakurai K, Shinkai S. Inclusion of cut and as-grown single-walled carbon nanotubes in the helical superstructure of schizophyllan and curdlan (beta-1,3-glucans). J Am Chem Soc. 2005;127:5875–84.
33. Numata M, Hasegawa T, Fujisawa T, Sakurai K, Shinkai S. β-1,3-Glucan (Schizophyllan) can act as a one-dimensional host for creation of novel poly(aniline) nanofiber structures. Org Lett. 2004;6:4447–50.
34. Sakurai K, Shinkai S. Molecular recognition of adenine, cytosine, and uracil in a single-stranded RNA by a natural polysaccharide: schizophyllan. J Am Chem Soc. 2000;122:4520–1.
35. Kasai N, Harada T. Ultrastructure of curdlan. In: French AD, Gardner KH (eds) Fiber diffraction methods. American Chemistry Society Symposium. American chemical society; 1980. Vol. 141 p. 363–383. https://pubs.acs.org/doi/abs/10.1021/bk-1980-0141.ch024.
36. Zhou X, Zhang X, Han S, Dou Y, Liu M, Zhang L, et al. Yeast microcapsule-mediated targeted delivery of diverse nanoparticles

for imaging and therapy via the oral route. Nano Lett. 2017;17:1056–64.
37. Xu S, Lin Y, Huang J, Li Z, Xu X, Zhang L. Construction of high strength hollow fibers by self-assembly of a stiff polysaccharide with short branches in water. J Mater Chem A. 2013;1:4198–206.
38. Liu Q, Xu X, Zhang L, Yu J. Interaction between polydeoxyadenylic acid and β-glucan from Lentinus edodes. Eur Polym J. 2012;48:1329–38.
39. Ikeda M, Hasegawa T, Numata M, Sugikawa K, Sakurai K, Fujiki M, et al. Instantaneous inclusion of a polynucleotide and hydrophobic guest molecules into a helical core of cationic β-1, 3-glucan polysaccharide. J Am Chem Soc. 2007;129:3979–88.
40. Sanada Y, Matsuzaki T, Mochizuki S, Okobira T, Uezu K, Sakurai K. β-1,3-D-glucan schizophyllan/poly (dA) triple-helical complex in dilute solution. J Phys Chem B. 2012;116:87–94.
41. Mizu M, Koumoto K, Anada T, Matsumoto T, Numata M, Shinkai S, et al. A polysaccharide carrier for immunostimulatory CpG DNAs to enhance cytokine secretion. J Am Chem Soc. 2004;126:8372–3.
42. Liu Q, Xu H, Cao Y, Li M, Xu X, Zhang L. Transfection efficiency and internalization of the gene carrier prepared from a triple-helical beta-glucan and polydeoxyadenylic acid in macrophage RAW264.7 cells. J Mater Chem B. 2015;3:3789–98.
43. Anada T, Karinaga R, Koumoto K, Mizu M, Nagasaki T, Kato Y, et al. Linear double-stranded DNA that mimics an infective tail of virus genome to enhance transfection. J Control Rel. 2005;108:529–39.
44. Duan B, Li M, Sun Y, Zou S, Xu X. Orally delivered antisense oligodeoxyribonucleotides of TNF-α via polysaccharide-based nanocomposites targeting intestinal inflammation. Adv Health Mater. 2019;8:1801389.
45. Zeng W, Zhang Z, Gao H, Jia L, Chen W. Characterization of antioxidant polysaccharides from Auricularia auricular using microwave-assisted extraction. Carbohydr Polym. 2012;89:694–700.
46. Li C, Mao X, Xu B. Pulsed electric field extraction enhanced anti-coagulant effect of fungal polysaccharide from Jew's ear (Auricularia auricula). Phytochem Anal. 2012;24:36–40.
47. Zhang L, Wang M. PEG-based ultrasound-assisted extraction of polysaccharides from superfine ground Auricularia auricular. J Food Process Pres. 2017;42:e13445.
48. Ma Y, Wang C, Zhang Q, Peng X, Feng Y, Meng X. The effects of polysaccharides from Auricularia auricula (Huaier) in adjuvant anti-gastrointestinal cancer therapy: a systematic review and network meta-analysis. Pharm Res. 2018;132:80–9.
49. Ma Z, Wang J, Zhang L. Structure and chain conformation of beta-glucan isolated from Auricularia auricula-judae. Biopolymers. 2008;89:614–22.
50. Ma Z, Zhang L, Nishiyama Y, Marais MF, Mazeau K, Vignon M. The molecular structure and solution conformation of an acidic heteropolysaccharide from Auricularia auricula-judae. Biopolymers. 2010;95:217–27.
51. Xu S, Xu X, Zhang L. Branching structure and chain conformation of water-soluble glucan extracted from Auricularia auricula-judae. J Agr Food Chem. 2012;60:3498–506.
52. Mapoung S, Umsumarng S, Semmarath W, Arjsri P, Thipprapphan P, Yodkeeree S, Limtrakul P. Skin wound-healing potential of polysaccharides from medicinal mushroom Auriculariaauricula-judae (Bull.). J Fungi. 2021;7:247.
53. Zhao R, Cheng N, Nakata PA, Zhao L, Hua Q. Consumption of polysaccharides from Auricularia auricular modulates the intestinal microbiota in mice. Food Res Int. 2019;123:383–92.
54. Meng Y, Shi X, Cai L, Zhang S, Ding K, Nie S, et al. Triple-helix conformation of a polysaccharide determined with light scattering, AFM, and molecular dynamics simulation. Macromolecules. 2018;51:10150–9.
55. Zhang L, Xue Q, Mo Z, Jin X. Modern research methods in polymer physics. Wuhan University Press; 2003. p. 11–76. http://www.wdp.com.cn/book/toBookInfoDetailPage.action?id=1531&flag=%20%20%20%20%20%204.
56. Itou T, Teramoto A. Ordered structure in aqueous polysaccharide. 5. cooperative order-disorder transition in aqueous schizophyllan. Macromolecules. 1986;19:1234–40.
57. Nardin R, Vincendon M. Isotopic exchange study of the scleroglucan chain in solution. Macromolecules. 1989;22:3551–4.
58. Kony DB, Damm W, Stoll S, Gunsteren WF, Hünenberger PH. Explicit-solvent molecular dynamics simulations of the polysaccharide schizophyllan in water. Biophys J. 2007;93:442–55.
59. Sakurai K, Uezu K, Numata M, Hasegawa T, Li C, Kaneko K, Shinkai S. β-1,3-Glucan polysaccharides as novel one-dimensional hosts for DNA/RNA, conjugated polymers and nanoparticles. Chem Comm. 2005;35:4383–98.
60. Chen N, Zhang H, Zong X, Li S, Wang J, Wang Y, Jin M. Polysaccharides from Auricularia auricula: preparation, structural features and biological activities. Carbohydr Polym. 2020;247:116750.
61. Liu E, Ji Y, Zhang F, Liu B, Meng XH. Review on Auricularia auricula-judae as a functional food: growth, chemical composition, and biological activities. J Agric Food Chem. 2021;69:1739–50.
62. Perera N, Yang FL, Chern J, Chiu HW, Hsieh CY, Li LH, et al. Carboxylic and o-acetyl moieties are essential for the immunostimulatory activity of glucuronoxylomannan: a novel TLR4 specific immunostimulator from Auricularia auricula-judae. Chem Commun. 2018;54:6995–8.
63. Bai HN, Wang ZY, Cui J, Yun KL, Zhang H, Liu RH, et al. Synergistic radiation protective effect of purified Auricularia auricular-judae polysaccharide (AAP IV) with grape seed procyanidins. Molecules. 2014;19:20675–94.
64. Ma Z, Wang J, Zhang L, Zhang Y, Ding K. Evaluation of water soluble β-d-glucan from Auricularia auricular-judae as potential anti-tumor agent. Carbohydr Polym. 2010;80:977–83.
65. Ping Z, Xu H, Liu T, Huang J, Meng Y, Xu X, et al. Anti-hepatoma activity of the stiff branched β-D-glucan and effects of molecular weight. J Mater Chem B. 2016;4:4565–73.
66. Cai L, Zhou S, Wang Y, Xu X, Zhang L, Cai Z. New insights into the anti- hepatoma mechanism of triple-helix β-glucan by metabolomics profiling. Carbohydr Polym. 2021;269:118289.
67. Zhang L, Xu X, Jiang G, Iijima H, Tsuchiya H. Aggregation of aeromonas gum in aqueous solution. Polym J. 1999;31:150–3.
68. Xu X, Zhang L. Aggregation and disaggregation of Aeromonas gum in an aqueous solution under different conditions. J Polym Sci Part B: Polym Phys. 2000;38:2644–51.
69. Zhang Y, Xu X, Zhang L. Gel formation and low-temperature intramolecular conformation transition of a triple-helical polysaccharide lentinan in water. Biopolymers. 2008;89:852–61.
70. Xu X, Xu J, Zhang Y, Zhang L. Rheology of triple helical lentinan in solution: steady shear viscosity and dynamic oscillatory behavior. Food Hydrocolloid. 2008;22:735–41.
71. Zhang Y, Xu X, Zhang L. Dynamic viscoelastic behavior of triple helical lentinan in water: effect of temperature. Carbohydr Polym. 2008;73:26–34.
72. Jin Y, Cai L, Yang Q, Luo Z, Liang L, Liang Y, et al. Anti-leukemia activities of selenium nanoparticles embedded in nanotube consisted of triple-helix β-D-glucan. Carbohydr Polym. 2020;240:116329.
73. Suntharalingam K, Song Y, Lippard SJ. Conjugation of vitamin E analog α-TOS to Pt (IV) complexes for dual-targeting anticancer therapy. Chem Commun. 2014;50:2465–68.
74. Gramatica P, Papa E, Luini M, Monti E, Gariboldi MB, Ravera M, et al. Antiproliferative Pt (IV) complexes: synthesis,

biological activity, and quantitative structure-activity relationship modeling. J Biol Inorg Chem. 2010;15:1157–69.
75. Chen K, Cai L, Yang S, Peng S, Huang J, Xu J, et al. Zhou X. Pt (IV) prodrugs designed to embed in nanotubes of a polysaccharide for drug delivery. ACS Appl Bio Mater. 2021;4:4841–8.
76. Sheng K, Wang C, Chen B, Kang M, Wang M, Liu K, et al. Recent advances in polysaccharides from Lentinus edodes (Berk.): isolation, structures and bioactivities. Food Chem. 2021;358:129883.
77. Xu X, Yan H, Tang J, Chen J, Zhang X. Polysaccharides in Lentinus edodes: isolation, structure, immunomodulating activity and future prospective. Crit Rev Food Sci. 2014;54:474–87.
78. Chihara G, Maeda Y, Hamuro J, Sasaki T, Fukuoka F. Inhibition of mouse sarcoma 180 by polysaccharides from Lentinus edodes (Berk.) sing. Nature. 1969;222:687–8.
79. Chihara G, Hamuro J, Maeda Y, Arai Y, Fukuoka F. Fractionation and purification of the polysaccharides with marked antitumor activity, especially lentinan, from Lentinus edodes (Berk.) Sing. (an edible mushroom). Cancer Res. 1970;30:2776–81.
80. Xu X, Chen P, Zhang L, Ashida H. Chain structures of glucans from Lentinus edodes and their effects on NO production from RAW 264.7 macrophages. Carbohydr Polym. 2012;87:1855–1862.
81. Lin Y, Zeng H, Wang K, Lin H, Li P, Huang Y, et al. Micro wave-assisted aqueous two-phase extraction of diverse polysaccharides from Lentinus edodes: process optimization, structure characterization and antioxidant activity. Int J Biol Macromol. 2019;136:305–15.
82. Tao Y, Zhang L, Yan F, Wu X. Chain conformation of water-insoluble hyperbranched polysaccharide from fungus. Biomacromolecules. 2007;8:2321–8.
83. Bian C, Xie N, Chen F. Preparation of bioactive water-soluble pachyman hydrolyzed from sclerotial polysaccharides of Poria cocos by hydrolase. Polym J. 2010;42:256–60.
84. Gidley M. Quantification of the structural features of starch polysaccharides by NMR spectroscopy. Carbohydr Res. 1985;139:85–93.
85. Liu Q, Xu X, Zhang L. Variable chain conformations of renatured β-glucan in dimethylsulfoxide/water mixture. Biopolymers. 2012;97:988–97.
86. Yoshiba K, Dobashi T, Ulset AST, Christensen BE. Cooperative order-disorder transition of carboxylated schizophyllan in water–dimethylsulfoxide mixtures. J Phys Chem B. 2018;122:6551–8.
87. Zhang Y, Gu M, Wang K, Chen Z, Dai L, Liu J, et al. Structure, chain conformation and antitumor activity of a novel polysaccharide from Lentinus edodes. Fitoterapia. 2010;81:1163–70.
88. Wang X, Zhang X, Xu X, Zhang L. The LiCl effect on the conformation of lentinan in DMSO. Biopolymers. 2012;97:840–5.
89. Zhang Y, Li S, Zhang L. Aggregation behavior of triple helical polysaccharide with low molecular weight in diluted aqueous solution. J Phys Chem B. 2010;114:4945–54.
90. Wang X, Zhang Y, Zhang L, Ding Y. Multiple conformation transitions of triple helical lentinan in DMSO/water by microcalorimetry. J Phys Chem B. 2009;113:9915–23.
91. Zhang X, Zhang L, Xu X. Morphologies and conformation transition of lentinan in aqueous NaOH solution. Biopolymers. 2004;75:187–95.
92. Wang X, Xu X, Zhang L. Thermally induced conformation transition of triple-helical lentinan in NaCl aqueous solution. J Phys Chem B. 2008;112:10343–51.
93. Wang J, Li W, Huang X, Liu Y, Li Q, Zheng Z. A polysaccharide from Lentinus edodes inhibits human colon cancer cell proliferation and suppresses tumor growth in athymic nude mice. Oncotarget. 2017;8:610–23.
94. Li W, Wang J, Hu H, Li Q, Liu Y, Wang K. Functional polysaccharide lentinan suppresses human breast cancer growth via inducing autophagy and caspase-7-mediated apoptosis. J Func Foods. 2018;45:75–85.
95. Wang X, Wang Y, Zhou Q, Peng M, Zhang J, Chen M, et al. Immunomodulatory effect of lentinan on aberrant T subsets and cytokines profile in non-small cell lung cancer patients. Pathol Oncol Res. 2020;26:499–505.
96. Vannucci L, Sima P, Vetvicka V, Krizan J. Lentinan properties in anticancer therapy: a review on the last 12-year literature. Am J Immunol. 2017;13:50–61.
97. Xu H, Zou S, Xu X. The β-glucan from Lentinus edodes suppresses cell proliferation and promotes apoptosis in estrogen receptor positive breast cancers. Oncotarget. 2017;8:86693–709.
98. Zheng X, Lu F, Xu X, Zhang L. Extended chain conformation of β-glucan and its effect on antitumor activity. J Mater Chem B. 2017;5:5623–31.
99. Zheng X, Zhou F, Xu X, Zhang L. Uptake of intraperitoneally administrated triple helical β-glucan for antitumor activity in murine tumor models. J Mater Chem B. 2017;5:9337–45.
100. Zou S, Duan B, Xu X. Inhibition of tumor growth by β-glucans through promoting CD4+ T cell immunomodulation and neutrophil-killing in mice. Carbohydr Polym. 2019;213:370–81.
101. Du B, Lin C, Bian Z, Xu B. An insight into anti-inflammatory effects of fungal beta-glucans. Trends Food Sci Tech. 2015;41:49–59.
102. Liu Y, Zhao J, Zhao Y, Zong S, Tian Y, Chen S, et al. Therapeutic effects of lentinan on inflammatory bowel disease and colitis-associated cancer. J Cell Mol Med. 2019;23:750–60.
103. Goodridge HS, Wolf AJ, Underhill DM. β-glucan recognition by the innate immune system. Immunol Rev. 2009;230:38–50.
104. Wang Y, Jin H, Yu J, Qu C, Wang Q, Yang S, et al. Quality control and immunological activity of lentinan samples produced in China. Int J Biol Macromol. 2020;159:129–36.
105. Xu X, Chen P, Zhang L, Ashida H. Immunomodulatory β-glucan from Lentinus edodes activates mitogen-activated protein kinases and nuclear factor-κB in murine RAW 264.7 macrophages. J Biol Chem. 2011;286:31194–8.
106. Zhang L, Li X, Xu X, Zeng F. Correlation between antitumor activity, molecular weight, and conformation of lentinan. Carbohydr Res. 2005;340:1515–21.
107. Surenjav U, Zhang L, Xu X, Zhang X, Zeng F. Effects of molecular structure on antitumor activities of (1→3)-β-D-glucans from different Lentinus edodes. Carbohydr Polym. 2006;63:97–104.
108. Ibrahim R, Hayyan M, AlSaadi M, Hayyan A, Ibrahim S. Environmental application of nanotechnology: air, soil, and water. Environ Sci Pollut Res. 2016;23:13754–88.
109. Seyedebrahimi R, Razavi S, Varshosaz J. Controlled delivery of brain derived neurotrophic factor and gold-nanoparticles from chitosan/TPP nanoparticles for tissue engineering applications. J Clust Sci. 2020;31:99–108.
110. He X, Deng H, Hwang H. The current application of nanotechnology in food and agriculture. J Food Drug Anal. 2019;27:1–21.
111. Jia X, Liu Q, Zou S, Xu X, Zhang L. Construction of selenium nanoparticles/β-glucan composites for enhancement of the antitumor activity. Carbohydr Polym. 2015;117:434–42.
112. Jia X, Xu X, Zhang L. Synthesis and stabilization of gold nanoparticles induced by denaturation and renaturation of triple helical β-glucan in water. Biomacromolecules. 2013;14:1787–94.

113. Li S, Zhang Y, Xu X, Zhang L. Triple helical polysaccharide-induced good dispersion of silver nanoparticles in water. Biomacromolecules. 2011;12:2864–71.
114. Jia X, Chen P, Xu X, Zhang L. Lentinan greatly enhances the dispersibility of single-walled carbon nanotubes in water and decreases the cytotoxicity. Bioact Carbohydr Diet Fibre. 2013;1:111–9.
115. Li M, Chen P, Xu M, Xu X. A novel self-assembly Lentinan-tetraphenylethylene composite with strong blue fluorescence in water and its properties. Carbohyd Polym. 2017;174:13–24.
116. Miyoshi K, Uezu K, Sakurai K, Shinkai S. Polysaccharide-Polynucleotide complexes. Part 32. Structural analysis of the curdlan/Poly (cytidylic acid) complex with semiempirical molecular orbital calculations. Biomacromolecules. 2005;6:1540–6.
117. Sakurai K, Mizu M, Shinkai S. Polysaccharide- polynucleotide complexes. 2. Complementary polynucleotide mimic behavior of the natural polysaccharide schizophyllan in the macromolecular complex with single-stranded RNA and DNA. Biomacromolecules. 2001;2:641–50.
118. Duan B, Zou S, Sun Y, Xu X. Nanoplatform constructed from a β-glucan and polydeoxyadenylic acid for cancer chemotherapy and imaging. Biomacromolecules. 2019;20:1567–77.
119. Duan B, Zou S, Sun Y, Xu X. Fabrication of tumor-targeting composites based on the triple helical β-glucan through conjugation of aptamer. Carbohydr Polym. 2021;254:117476.
120. Gallone B, Steensels J, Prahl T, Soriaga L, Saels V, Herrera-Malaver B, et al. Domestication and divergence of Saccharomyces cerevisiae beer yeasts. Cell. 2016;166:1397–410.
121. Samuelsen A, Schrezenmeir J, Knutsen SH. Effects of orally administered yeast-derived beta-glucans: a review. Mol Nutr Food Res. 2014;58:183–93.
122. Lipke PN, Ovalle R. Cell wall architecture in yeast: new structure and new challenges. J Bacteriol. 1998;180:3735–40.
123. Osumi M. The ultrastructure of yeast: cell wall structure and formation. Micron. 1998;29:207–33.
124. EFSA Panel on Dietetic Products, Nutrition and Allergies (NDA). Scientific opinion on the safety of 'yeast beta-glucans' as a novel food ingredient. EFSA J. 2011;9:2137.
125. Sun Y, Shi X, Zheng X, Nie S, Xu X. Inhibition of dextran sodium sulfate-induced colitis in mice by baker's yeast polysaccharides. Carbohydr Polym. 2019;207:371–81.
126. Li H, Wang W, Hou K, Huang Y, Gao L. Autolysis-ultrasonic coupling extraction of β-1,3-D-glucan from waste beer yeast. Fine Chem. 2014;31:96–9.
127. Fleet GH, Manners DJ. The enzymic degradation of an alkali-soluble glucan from the cell walls of saccharomyces cerevisiae. J Gen Microbiol. 1977;98:315–27.
128. Smet RD, Cuvelier CA, Allais LH. Recent advances in oral vaccine development yeast-derived β-glucan particles. Hum Vacc Immunother. 2014;10:1309–18.
129. Manners DJ, Masson AJ, Patterson JC. The structure of a β-(1→3)-D-glucan from yeast cell walls. Biochem J. 1973;135:19–30.
130. Kollar RR, Reinhold BB, Petráková EE, Yeh H, Cabib E. Architecture of the yeast cell wall. β-(1–>6)-glucan interconnects mannoprotein, β-(1–>3)-glucan, and chitin. J Biol Chem. 1997;272:17762–75.
131. Hisamatsu M, Mishima T, Teranishi K, Yamada T. The correlation between adhesion of schizophyllan to yeast glucan and its effect on regeneration of yeast protoplast. Carbohydr Res. 1997;298:117–21.
132. Krainer E, Stark RE, Naider F, Alagramam K, Becker JM. Direct observation of cell wall glucans in whole cells of saccharomyces cerevisiae by magic-angle spinning ^{13}C-NMR. Biopolymers. 1994;34:1627–35.
133. Williams DL, Pretus HA, Ensley HE, Browder IW. Molecular weight analysis of a water-insoluble, yeast-derived (1→3)-β-D-glucan by organic-phase size-exclusion chromatography. Carbohydr Res. 1994;253:293–8.
134. Soto E, Yun SK, Lee J, Kornfeld H, Ostroff G. Glucan particle encapsulated Rifampicin for targeted delivery to macrophages. Polymers. 2010;2:681–9.
135. Soto E, Ostroff G. Oral macrophage mediated gene delivery system. NSTI Nanotech. 2007;2:378–81.
136. Sabu C, Mufeedha P, Pramod K. Yeast-inspired drug delivery: biotechnology meets bioengineering and synthetic biology. Expert Opin Drug Deliv. 2019;16:27–41.
137. Stier H, Ebbeskotte V, Gruenwald J. Immune-modulatory effects of dietary yeast beta-1,3/1,6-D-glucan. Nutr J. 2014;13:38.
138. Pillemer L, Blum L, Lepow IH, Wurz L, Todd EW. The properdin system and immunity. III. The zymosan assay of properdin. J Exp Med. 1956;103:1–13.
139. Dambuza IM, Brown GD. C-type lectins in immunity: recent developments. Curr Opin Immunol. 2015;32:21–7.
140. Brown GD. Dectin-1: a signalling non-TLR pattern-recognition receptor. Nat Rev Immunol. 2006;6:33–43.
141. Reid DM, Gow NA, Brown GD. Pattern recognition: recent insights from dectin-1. Curr Opin Immunol. 2009;21:30–7.
142. Herre J, Marshall AS, Caron E, Edwards AD, Williams DL, Schweighoffer E, et al. Dectin-1 uses novel mechanisms for yeast phagocytosis in macrophages. Blood. 2004;104:4038–45.
143. Graaff P, Govers C, Wichers HJ, Debets R. Consumption of β-glucans to spice up T cell treatment of tumors: a review. Expert Opin Biol Ther. 2018;18:1023–40.
144. Cousens LP, Orange JS, Su HC, Biron CA. Interferon-α/β inhibition of interleukin 12 and interferon-γ production in vitro and endogenously during viral infection. Proc Natl Acad Sci USA. 1997;94:634–9.
145. Xu X, Yasuda M, Mizuno M, Ashida H. β-Glucan from Saccharomyces cerevisiae reduces lipopolysaccharide-induced inflammatory responses in RAW264.7 macrophages. BBA Gen Subj. 2012;1820:1656–63.
146. Cao Y, Sun Y, Zou S, Duan B, Sun M, Xu X. Yeast β-glucan suppresses the chronic inflammation and improves the microenvironment in adipose tissues of ob/ob mice. J Agric Food Chem. 2018;66:621–9.
147. Albeituni SH, Ding C, Liu M, Hu X, Luo F, Kloecker G, et al. Yeast-derived particulate β-glucan treatment subverts the suppression of myeloid-derived suppressor cells (MDSC) by inducing polymorphonuclear MDSC apoptosis and monocytic MDSC differentiation to APC in cancer. J Immunol. 2016;196:2167–80.
148. Ning Y, Xu D, Zhang X, Yu B, Qi C. β-Glucan restores tumor-educated dendritic cell maturation to enhance antitumor immune responses. Int J Cancer. 2016;138:2713–23.
149. Min L, Luo F, Ding C, Albeituni S, Yan J. Dectin-1 activation by a natural product β-glucan converts immunosuppressive macrophages into an M1-like phenotype. J Immunol. 2015;196:5055–65.
150. Choi J, Kim H, Jung, Hong S, Song J. Consumption of barley β-glucan ameliorates fatty liver and insulin resistance in mice fed a high-fat diet. Mol Nutr Food Res. 2010;54:1004–13.
151. Chen J, Raymond K. Beta-glucans in the treatment of diabetes and associated cardiovascular risks. Vasc Health Risk Man. 2008;4:1265–72.
152. Cao Y, Zou S, Xu H, Li M, Tong Z, Xu M, Xu X. Front cover: Hypoglycemic activity of the baker's yeast β-glucan in obese/type 2 diabetic mice and the underlying mechanism. Mol Nutr Food Res. 2016;60:2678–90.
153. Cao Y, Sun Y, Zou S, Li M, Xu X. Orally administered baker's yeast β-glucan promotes glucose and lipid homeostasis in the

livers of obesity and diabetes model mice. J Agric Food Chem. 2017;65:9665–74.
154. Garello F, Stefania R, Aime S, Terreno E, Castelli DD. Successful entrapping of liposomes in glucan particles: an innovative micron-sized carrier to deliver water-soluble molecules. Mol Pharm. 2014;11:3760–5.
155. Sun Y, Duan B, Chen H, Xu X. A novel strategy for treating inflammatory bowel disease by targeting delivery of methotrexate through glucan particles. Adv Health Mater. 2020;9:1901805.
156. Soto ER, Ostroff GR. Characterization of multilayered nanoparticles encapsulated in yeast cell wall particles for DNA delivery. Bioconjugate Chem. 2008;19:840–8.
157. Aouadi M, Tesz GJ, Nicoloro SM, Wang M, Chouinard M, Soto E, et al. Orally delivered siRNA targeting macrophage Map4k4 suppresses systemic inflammation. Nature. 2009;458:1180–84.
158. Liu H, Jia Z, Yang C, Song M, Jing Z, Zhao Y, et al. Aluminum hydroxide colloid vaccine encapsulated in yeast shells with enhanced humoral and cellular immune responses. Biomaterials. 2018;167:32–43.

Huanhuan Chen received her MS degree from College of Food Science and Technology, Huazhong Agricultural University in 2019, majoring in Food Science. Currently, she is studying as a PhD student in Wuhan University under the supervision of Prof. Xiaojuan Xu. Her research focuses on the fabrication of biomaterial based on yeast β-glucan and its biomedical applications.

Ningyue Liu received her MS degree from Northeast Agricultural University in 2019. Currently, she is studying as a PhD student in Wuhan University under the supervision of Prof. Xiaojuan Xu. She is currently working on the biological activity of β-glucan from *Lentinus edodes* and its potential mechanism.

Fangzhou He received her BS degree from the College of Chemistry, Central China Normal University in 2020. Currently, she is studying for her MS degree in Wuhan University under the supervision of Prof. Xiaojuan Xu. Her reasearch focuses on the modification of yeast β-glucan and its biomedical materials construction.

Qingye Liu received his PhD degree from Wuhan University in 2014 under the supervision of Prof. Xiaojuan Xu, and after that he joined the North University of China. He spent two and half years (2016-2019) in Texas Tech University as a postdoctoral fellow for designing chitosan-derived hydrogel materials. Now he is currently an associate professor in North University of China. His research interests mainly focus on the naturally-derived smart materials for drug/gene delivery, and functional hydrogel materials in tissue engineering.

Prof. Xiaojuan Xu is currently a professor in College of Chemistry and Molecular Sciences at Wuhan University. She received her BS degree in 1997 and PhD in 2002 from Wuhan University, and joined Wuhan University in 2001. She spent one year (2000-2001) in Osaka University working on polysaccharide solutions, and two years (2008-2010) in Kobe University as a JSPS postdoctoral fellow for the investigation of structure-bioactivity correlation of polysaccharides. Her research interests focus on chemical structure, chain conformation, and biological functions of natural polysaccharides, as well as the development of polysaccharide-based nanocomposites for biomedical applications as drug/gene delivery carriers.